이학박사 학위논문

Applications of ^{3}H and ^{7}Be as tracers of atmospheric water vapor and particles

^{3}H과 ^{7}Be을 이용한 대기 수증기 및 입자 추적

2019년 2월

서울대학교 대학원

지구환경과학부

채 정 석

Ph.D. Dissertation of science

Applications of ^{3}H and ^{7}Be as tracers of atmospheric water vapor and particles

^{3}H과 ^{7}Be을 이용한 대기 수증기 및 입자 추적

February 2019

School of Earth and Environmental Sciences
Seoul National University

Jung Seok Chae

Abstract

Applications of ^{3}H and ^{7}Be as tracers of atmospheric water vapor and particles

Jung Seok Chae

The naturally or artificially produced ^{3}H (tritium) and cosmogenic ^{7}Be have been extensively applied to investigate the various environment processes in atmosphere and hydrosphere due to the similar behavior, physical and chemical properties to hydrogen constituting water for tritium and the particle reactive characteristics for ^{7}Be, and their suitable half-life. The main goals of this study are the investigation and application of tritium and ^{7}Be to construct an important index of tritium levels in precipitation for ground water age dating, determine the seasonal variations in removal efficiency of fine aerosols in the Northeast Asia using cosmogenic ^{7}Be, and evaluate the dispersion and removal characteristics of tritium originated from nuclear power plants in the atmosphere.

Several studies have documented the characteristics of seasonal, decadal, and horizontal variations of tritium in different regions including North America, Australia, and Europe. However, long-term data such as these studies were not yet reported for Northeast Asia. In this study, we document the extensive spatial-temporal monitoring data of tritium levels in precipitation measured at 16 stations in Korea over the last 20 years, including the long-term trend since 1961 by using measured and estimated data. The long-term variation of tritium concentrations in

the Korean precipitation follows the global trend, reaching the maximum in 1963 owing to nuclear bomb testing, followed by a consistent level since the late 1990s. Tritium concentrations in precipitation from 1998 to 2017 were maximum in spring (April) due to tropopause folding and minimum in summer (July) due to the dominant inflows of marine air. The tritium concentrations in precipitation were lower toward the coastal stations, due to the influence of marine moisture for all seasons. Our results characterize the differences in tritium levels in recharging areas, for different periods in this region. Therefore, these results will serve as an important index of hydrological cycles of tritium in Northeast Asia, which is important for understanding global hydrological cycles.

To determine the seasonal variations in the removal efficiency of fine aerosols in the Northeast Asia, we analyzed ^{7}Be data collected for the surface air and precipitation over 20 years in Korea. The ^{7}Be concentrations in the surface air were relatively higher in spring owing to tropopause folding but lower in summer owing to efficient removal by precipitation. The monthly ^{7}Be activities decreased as the precipitation amounts increased, while showing a correlation (r^2=0.34) against the precipitation amount. The ^{7}Be activities also showed a positive correlation (r^2=0.32) with PM10. These results indicate that the concentrations of ^{7}Be and PM10 are mainly controlled by the same washout effect, although the sources are different. The mean depositional velocities of fine aerosols, based on the ^{7}Be mass balance model, showed a large seasonal variation, with its maximum value (1.9 cm s^{-1}) in July and minimum value (0.22 cm s^{-1}) in March. This result suggests that the concentrations as high as six-fold in PM10 can occur in the dry season (winter), if the input terms remain the same. Our results imply that precipitation plays a critical role in the seasonal changes in the concentrations of fine aerosols, providing much clean air in

the summer monsoon season in the Northeast Asia.

The activities of tritium in water-vapor (n = 649) and precipitation (n = 2404) samples were measured from 1998 to 2015 around the Wolsong nuclear power plant (NPP) site where four pressurized heavy water reactors and two pressurized water reactors operated. The activity concentrations of tritium in the water-vapor and precipitation samples were in the ranges of 2.2–2200 Bq/L and 0.3–1090 Bq/L, respectively. The concentrations in spring were approximately 7 times higher than those in fall and winter, mainly owing to the wind directions at the power plant locations. The annual geometric mean activities of tritium in the water-vapor and precipitation samples varied within 56% and 83% from the average, respectively, depending primarily on the annual discharge amount of tritium to the atmosphere. The activities of tritium in the water-vapor and precipitation samples rapidly decreased away from the power plant. Approximately 0.5–30% of tritium discharged from the NPP site was removed by precipitation to the ground within an area with a radius of 30 km from the NPP site, which linearly depended on the precipitation amount. Our results suggest that the wind direction and precipitation, in addition to the amount of discharge, are important factors that control the tritium concentrations in air near the NPP site.

Keywords : Tritium, Water vapor, Precipitation, ^{7}Be, Wet deposition, Aerosol

Student Number : 2011-30923

Table of Contents

List of Tables

List of Figures

1. General Introduction

1.1. Tritium

Physical characteristics

Hydrogen has three isotopes which are 1) protium, ^{1}H, the most abundant isotope of hydrogen (99.985%), 2) deuterium (0.015%), ^{2}H, and 3) tritium (trace), ^{3}H, the heaviest radioactive isotope of hydrogen. The tritium atom has one proton and two neutrons in its nucleus and one electron. The physical properties of tritium are similar to those of hydrogen (^{1}H). Tritium has a high diffusion coefficient. It willingly diffuses through porous substances such as rubber and can also diffuse through metal. Tritium, like common hydrogen, easily undergoes various chemical reactions depending on physical and chemical conditions. The common form of tritium in nature is tritium oxide (T_2O) or HTO. Tritium is widely distributed throughout the environment due to its ubiquitous form.

Radiological characteristics

The nucleus of the tritium atom is unstable and decays with the emission of a beta particle with mean energy of 5.7 keV and a maximum energy of 18.6 keV.

$$^{3}H \rightarrow {}^{3}He^{+} + e^{-} + \bar{\nu}_e$$

Tritium is a pure beta emitter with half-life of 12.32 years (Lucas and Unterweger, 2000). In water, the maximum track length of the beta particle is 6 μm (averaged 0.56 μm), which compares with a typical cell nucleus diameter of 6-15 μm, while the diameter of a cell are ranged from 10 μm to 100 μm. The beta particles do not penetrate dead layers of skin. However, following intake of tritium, beta radiation can irradiate internal organs.

Tritium production

Tritium is continually produced naturally in the upper layers of the atmosphere by interaction of high energy cosmic rays with the atmospheric gases. Tritium is mainly produced via the fast neutron interaction with nitrogen and oxygen in the atmosphere.

$$^{14}_{7}N + {}^{1}n \rightarrow {}^{12}_{6}C + {}^{3}_{1}H$$

$$^{16}_{8}O + {}^{1}n \rightarrow {}^{14}_{7}N + {}^{3}_{1}H$$

Cosmic ray-induced spallation reactions produce 7.2 x 10^{16} Bq of tritium per year (UNSCEAR, 2000). Another, very small, fraction of natural tritium is produced by neutron capture by ^{6}Li in the earth's crust. Tritium produced by natural processes is rapidly converted into HTO, which then joins the hydrological cycle. For this reason tritium has been widely used as a tracer in a variety of study fields such as hydrology, meteorology, oceanography, and meteorology.

Tritium is also produced artificially by nuclear weapon testing, operation of nuclear facilities, and nuclear accident. Significant quantities of tritium have been dispersed to the environment during the above-ground testing of nuclear weapons in the mid-1950s and early 1960s. The total amount of tritium released into the atmosphere by nuclear weapon testing from 1945 to 1980 was estimated to be 186,000 PBq. The quantity of tritium in the atmosphere from nuclear weapon testing peaked in 1963. Since the Partial Test Ban Treaty in 1963, the tritium level has declined. Nowadays, the levels of tritium in the atmosphere have almost reached to the levels of the pre-testing era (Guetat et al., 2011). Tritium has been released into the environment by operation of nuclear facilities. A large amount of tritium is

produced in heavy-water-moderated nuclear reactors through neutron capture by deuterium atoms. The global annual average releases of tritium to the atmosphere and to the aqueous environments from nuclear facilities were estimated to be 11.7 PBq and 16.0 PBq, respectively from 1998 to 2002.

Distribution of tritium

The inventory decreases by 5.5% per year through radioactive decay and some of the tritium leaks into the troposphere from where it is lost into the ocean or groundwater, both of which can be considered a sink for the stratospheric tritium. Tritium generally shows a higher concentration in the northern hemisphere than in the southern hemisphere due to the large number of nuclear weapon testing stations in the northern hemisphere and slow inter-hemispheric air transport. Tritium concentrations and inventories are dominated by the timing, location and intensity of exchange of tropospheric and stratospheric air masses. Exchange occurs predominantly during late winter and in spring in the region of tropopause discontinuities of the mid-latitudes.

Atmospheric movement of tritium

The main chemical forms of tritium in the atmosphere are, in order of importance: tritiated water vapor (HTO), tritium gas (HT) and tritiated methane. Because tritium levels in the atmosphere are not high enough to imply density effects, the tritium follows the air flows and is diluted by atmospheric dispersion like any other trace element. The removal processes of tritium are classified as wet deposition or dry deposition. Dry deposition occurs on contact with tritiated air via processes of collection through leaf epidermis or the ground. Wet deposition results from

scrubbing of the air by rain, snow and fog. Due to its low solubility, tritium in gaseous form HT and tritiated methane are rather concerned by dry deposition whereas the tritiated water vapor could be either deposited directly on the soil or contained in the raindrops.

1.2. ^{7}Be

Origin

Beryllium-7 (^{7}Be) is a relatively short-lived (half-life: 53.3 days) naturally occurring cosmogenic radionuclide formed by spallation processes of light atmospheric nuclei, such as carbon, nitrogen, and oxygen, when they absorb protons and even neutrons of the primary component of cosmic radiation, according to the following reactions:

$$^{12}C + p \rightarrow {}^{7}Be + {}^{6}Li \qquad ^{12}C + n \rightarrow {}^{7}Be + {}^{6}He$$

$$^{14}N + p \rightarrow {}^{7}Be + 2{}^{4}He \qquad ^{14}N + n \rightarrow {}^{7}Be + {}^{8}Li$$

$$^{16}O + p \rightarrow {}^{7}Be + {}^{10}B \qquad ^{16}O + n \rightarrow {}^{7}Be + {}^{10}Be$$

$$^{16}O + p \rightarrow {}^{7}Be + {}^{7}Li + {}^{3}He \qquad ^{16}O + n \rightarrow {}^{7}Be + {}^{6}He + {}^{4}He$$

^{7}Be is produced mainly in the stratosphere (70%), though it is also produced in the troposphere (30%). The production rates of ^{7}Be increase with increasing latitude. The rate of production decreases by about two orders of magnitude between the lower stratosphere and the surface air. The production rates of ^{7}Be vary with the 11 year sunspot cycle.

Behavior

Once ^{7}Be is produced in the troposphere, it rapidly associates primarily with submicron-sized aerosol particles. Beryllium-7 participates in the formation and growth of the accumulation mode aerosols (0.07 to 2 μm diameter), which are a major reservoir of atmospheric pollutants. Following ^{7}Be production, this isotope condenses on the aerosol population, growing by condensation of non-radioactive species such as H_2SO_4 or organics. About 88% of ^{7}Be was found to be present as

particles smaller than 1.1 μm in diameter, and less than 1% was on particles larger than 7 μm in diameter. ^{7}Be in these fine aerosols may subsequently enter the terrestrial and marine environment and vegetation via wet or dry depositional events. It is therefore susceptible to the same transport and deposition processes governing the aerosol, making it a useful atmospheric tracer. Beryllium-7 has been widely used as a potential tool in studying the description of environmental processes such as aerosol transit and residence times in the troposphere, aerosol deposition velocities.

Variation in the surface air

Low average concentrations are reported at high latitude sites, as well as at sites in the Pacific under the intertropical convergence zone. Higher average concentrations generally occur at middle latitudes of the Northern Hemisphere. Previous study found that seasonal variations showed the effects of at least four factors: (1) stratosphere-to-troposphere exchange; (2) vertical mixing within the troposphere; (3) air mass transport from middle to high latitudes; and (4) rainfall. The solar modulation of cosmic-ray fluxes also causes low frequency variations in the concentration of ^{7}Be in surface air. These variations are noticeable in measurements made over extended periods and show an anti-correlation with sunspot number.

Deposition

^{7}Be-bearing aerosols can reach the ground under clear sky conditions through particle sedimentation (dry deposition), but are removed more efficiently from the troposphere by precipitation scavenging (wet deposition). Experimental measurements show that around 90% or more of total ^{7}Be deposition in temperate

zones generally takes place through the wet deposition process. Wet deposition of ^{7}Be occurs through both below-cloud scavenging (washout) and in-cloud scavenging (rainout) of its carrier aerosol during a precipitation event. Washout occurs during the early stages and quickly cleanses the lower troposphere of ^{7}Be-bearing aerosols. Rainout delivers ^{7}Be from within the cloud layer to Earth's surface and is active throughout the duration of a precipitation event.

Annual deposition of ^{7}Be worldwide ranges from around 400 to 6500 Bq/m^{2} and appears to be dependent upon rainfall. Low annual depositions of this radionuclide have been reported for sites in the Middle East and Mediterranean regions, as well as at East Antarctica. The highest annual deposition of ^{7}Be to be reported (6350 Bq/m^{2}) is for a high rainfall area on the South Island of New Zealand.

^{7}Be depositional fluxes at different locations show a high positive correlation with rainfall, and temporal variations in the depositional flux of this radionuclide generally follow the local rainfall pattern. The deposition velocity of ^{7}Be-bearing aerosols can be calculated from the ratio of the ^{7}Be depositional flux to its concentration in surface air. Average deposition velocities of this radionuclide at different locations, including over the Pacific and Atlantic oceans, are reported to be in the range from 0.004 to 0.074 m s^{-1}.

1.3. Aim of this study

Tritium and ^{7}Be in precipitation, aerosol and water vapor in the surface air were measured throughout South Korea, located in Northeast Asia in order to investigate the behaviors of tritium and ^{7}Be in the atmosphere and understand the removal characterization of particulate matter from the surface atmosphere to the Earth's surface. The specific objectives of this study are:

(1) to characterize the variations of tritium concentrations in precipitation, which can be used as an index of tritium age dating in groundwater

(2) to determine the factors controlling temporal and spatial variations of tritium

(3) to determine the seasonal variations in the removal efficiency of fine aerosols in the Northeast Asia using ^{7}Be as an atmospheric tracer

(4) to evaluate the dispersion characteristics and removal proportions to the ground by precipitations for tritium released from the nuclear power plants

2. Seasonal and spatial variations of tritium in precipitation in Northeast Asia (Korea) over the last 20 years

2.1. Introduction

Tritium is the only radioisotope of hydrogen with the half-life of 12.32 years (Lucas and Unterweger, 2000). It is naturally produced by cosmic-ray spallation of nitrogen in the upper atmosphere (Craig and Lal, 1961). Two-thirds of this naturally occurring tritium is produced in the stratosphere and one-third in the troposphere. The natural production rate was estimated to be about 70 PBq/y for the whole atmosphere (Araguas et al., 1996). Tritium is supplied from the stratosphere to the troposphere mainly due to the elevation of tropopause height, called spring leak of the tropopause (Clark and Fritz, 1997; Gat et al., 2001; Yasunari and Yamazaki, 2009). Tritium can also be produced artificially by a variety of nuclear activities. The amount of tritium released into the atmosphere by the nuclear weapons testing from 1945 to 1980 was estimated to be around 200 EBq, which resulted in a factor of nearly 1000 higher level in 1963 in the Northern Hemisphere (Begemann and Libby, 1957; IAEA/WMO, 2018; Martell, 1963; Michel, 1976; Miskel, 1971; UNSCEAR, 2016). Nowadays the tritium concentration in precipitation reached the natural tritium level (Guetat et al., 2011). However, there are additional artificial sources of tritium from the routine operations of nuclear facilities; the amount of which is approximately tens of PBq each year (CNSC, 2009; UNSCEAR, 1988).

The tritium in the troposphere is removed to land or ocean through precipitation and eventually enters the hydrological cycle of the environment (Ehhalt et al., 2002; Morishima et al., 1985). Therefore, tritium has been used as a tracer in various fields including hydrological studies concerning ground water movement (Santschi et al., 1987; Solomon et al., 1992; Von Buttlar and Wendt, 1958), atmospheric and meteorological studies (Cauquoin et al., 2015; Moon et al., 1992; Rozanski et al., 1991; Yasunari and Yamazaki, 2009), and ocean circulation and ventilation (England and Maier-Reimer, 2001; Fine et al., 1981; Jenkins, 1996; Sarmiento, 1983). For dating tritium ages of modern groundwater, it is very important to know the initial tritium concentrations in precipitation.

Extensive data reports have been made in different regions of the world. Tritium in precipitation samples have been investigated by the Global Network of Isotopes in Precipitation (GNIP), which was created by the International Atomic Energy Agency (IAEA) and the World Meteorological Organization (WMO) in 1958. The GNIP includes more than 1,000 sampling stations over 125 countries (IAEA, 2018). The tritium data reports are available some major regions including Australia (1962-2012) (Tadros et al., 2014), Ottawa (Canada, 1953-2016) (IAEA, 2018), Ramnicu Valcea (Romania, 1999-2016) (Duliu et al., 2018), Hanoi (Vietnam, 2011-2016) (Anh et al., 2018), and Fukuoka (Japan,1987–1991) (Matsuoka et al., 1994). However, the long-term data (before 1963 to present) have not yet reported in the Northeast Asia, in spite of this region being important for global hydrological cycles in terms of human perturbations.

Thus, in this study, we present the long-term data of tritium in precipitation collected from nationwide monitoring stations from 1998 to 2017 throughout South Korea. The objective of this study is to characterize the variations of tritium concentrations in precipitation, which can be used as an index of tritium age dating in groundwater and to determine the factors controlling temporal and spatial variations of tritium in this region. In this study, we provide conversion factors of tritium concentration, the tritium values relative to the Korean stations, for different regions in East Asia.

2.2. Materials and Methods

2.2.1. Study area

The study area, South Korea, is located in the Northeast Asia. The Korean peninsula is mountainous and surrounded by marginal seas (Figure 2.1). This region is characterized by a humid continental and humid subtropical climate. The annual average precipitation ranges from 826 mm to 2007 mm and has regional differences (KMA, 2012). Since this peninsula is affected by the East Asian monsoon, most of the annual precipitation occurs in summer. Korea has four distinct seasons: spring (March–May), summer (June–August), autumn (September–November), and winter (December–February). Precipitation samples were collected at 16 sampling stations nationwide. Nine stations are located inland, four stations are located on the coastal areas, and three stations are located on the islands. The detailed information on the locations of sampling stations and sampling periods are shown in Table 2.1.

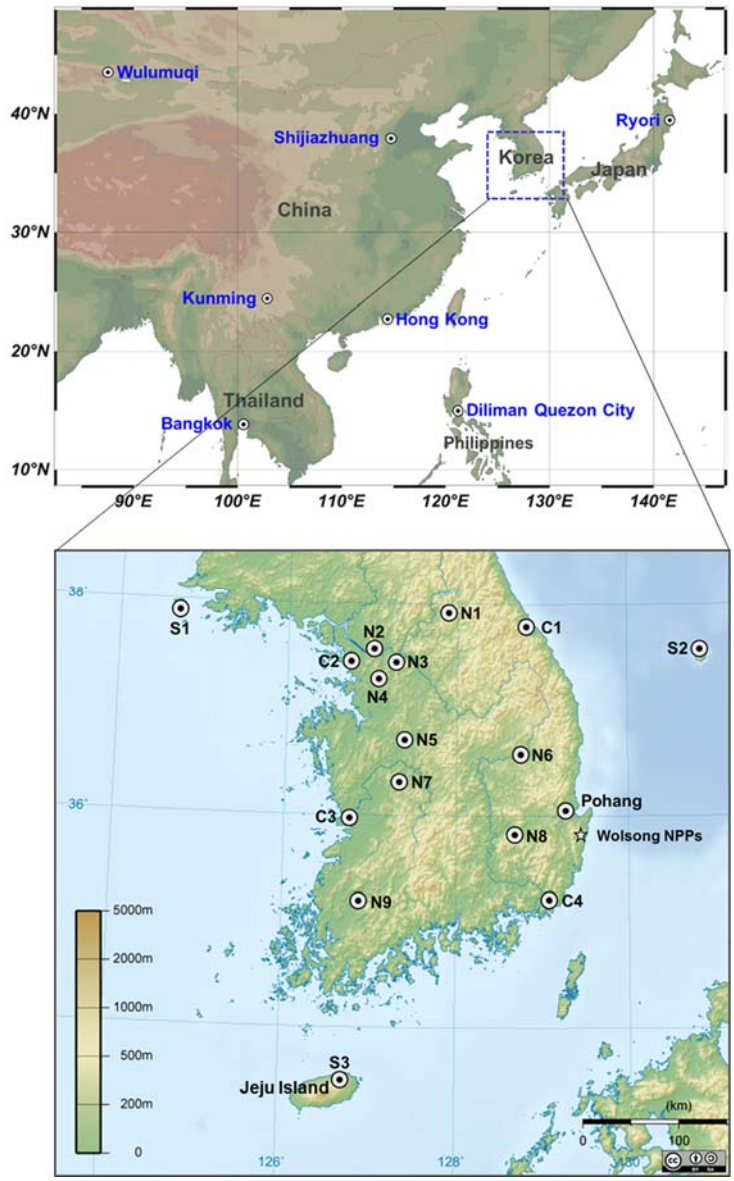

Figure 2.1. Map of sampling stations for tritium in precipitation in Korea. Stations S1–S3 are located in islands, stations C1–C4 are in coastal regions, and stations N1–N9 are in inland regions. This map was modified from the original map created by Ksiom.

Table 2.1. Sampling periods, latitude, longitude, and the number of samples for each sampling station in Korea.

Station ID	Location	Latitude (°N)	Longitude (°E)	Altitude (m)	n[a]	Period
N1	Chuncheon	37.8	127.7	119	162	1998-2011
N2	Seoul	37.5	127.0	25	159	1998-2011
N3	Seongnam	37.4	127.1	50	104	2003-2011
N4	Suwon	37.2	127.0	82	98	2003-2011
N5	Cheongju	36.6	127.4	84	99	2003-2011
N6	Andong	36.5	128.7	123	150	1998-2011
N7	Daejeon	36.3	127.3	51	230	1998-2017
N8	Daegu	35.8	128.6	48	154	1998-2011
N9	Gwangju	35.1	126.9	54	163	1998-2011
C1	Gangneung	37.7	128.8	31	158	1998-2011
C2	Incheon	37.4	126.7	10	56	1998-2002
C3	Gunsan	35.9	126.6	14	162	1998-2011
C4	Busan	35.1	129.1	9	148	1998-2011
S1	Baengnyeong	37.9	124.7	32	148	1998-2011
S2	Ulleung	37.4	130.8	140	153	1998-2011
S3	Jeju	33.4	126.5	285	159	1998-2011

2.2.2. Data acquisition and analyses

The tritium concentrations in precipitation samples from 16 nationwide monitoring stations throughout South Korea are available in the annual reports published by the Korea Institute of Nuclear Safety (KINS) (KINS, 1998-2017). The data of precipitation amounts were obtained from KMA database (KMA, 2018). The tritium data in precipitation measured in the world used in this study, including Pohang station in Korea, were obtained from the GNIP database (IAEA/WMO, 2018).

At Pohang station of GNIP, the oldest monitoring station in Korea, tritium in precipitation was measured from 1961 to 1976 (n=139). From 1998 to 2017, tritium concentrations in precipitation samples (n=2386) were measured at 16 monitoring stations (Figure 2.1). Since the monitoring data between 1977 and 1997 are not available, tritium concentrations in precipitation during this period were interpolated using the correlation between monitoring data from the southern part of the Korean Peninsula (Monitoring data from Pohang station, 1961–1976; Average values of monitoring data from stations of C1, C2, C3, and C4, 1998–2011) and those at Ottawa station in Canada, 1953–2016) (Figure 2.2).Ottawa station is one of the long running GNIP monitoring stations where up to the latest (2016) measurement data are available. The correlation equation can be presented as:

$$\ln(C_k) = 1.0171 \times \ln(C_o) - 1.1133 \quad (r^2=0.98;\ n=30)$$

where C_k is the estimated tritium value in the study region, and C_o is the monitoring result at Ottawa station. The data presented for the annual mean tritium concentration

in precipitation was weight normalized by the amount of precipitation using the method described in technical report published by IAEA (IAEA, 1992). Tritium concentrations in precipitation are presented as a tritium unit, where 1 TU corresponds to 0.11919 ± 0.00021 Bq kg^{-1} of water (Gröning and Rozanski, 2003).

The analytical methods used for monitoring are briefly described. Precipitation samples were collected monthly for 20 years. These precipitation samples were then distilled, and electrolytic enrichment was performed. After pretreatment, 10 mL of the water sample was added to a 20-mL Perfluoroalkoxy (PFA) vial, together with 10 mL of Ultima gold LLT cocktail (Packard, USA), and then sufficiently mixed. The prepared sample was measured using a liquid scintillation counter (1220 Quantulus, PerkinElmer). The minimum detectable activity and analytical uncertainty were estimated to be about 0.1 Bq/L and 5% (0.4TU), respectively. Since 1998, almost consistent methods for tritium analysis have been used without critical modifications.

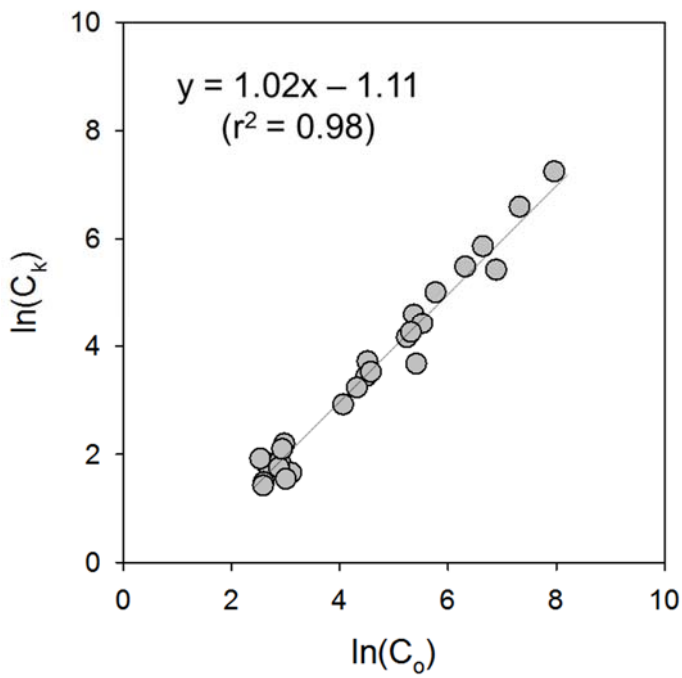

Figure 2.2. The correlation between monitoring data from the southern part of the Korean Peninsula (Station Pohang, 1961-1976; Station C4, 1998-2011) and those at Ottawa station in Canada (1953-2016).

2.3. Results and Discussion

2.3.1. Seasonal and spatial variations of tritium in precipitation

The monthly average tritium concentrations showed seasonal variations with the maximum values obtained in early spring (March–April) and minimum values obtained in late summer (July–August) at most of the sampling stations (Figure 2.3–2.5). The monthly tritium concentrations from 2003 to 2011 showed the standard deviation (SD) from 1.2 TU (St. S1) to 6.2 TU (St. N8). In general, in spring, the height of the tropopause increases, caused by the heating of the continental surface, and this process can lead to the transport of tritium-enriched air to the troposphere (Gat et al., 2001; Rozanski et al., 1991). In contrast, the decreased tritium concentrations in summer are attributed to the inflows of marine air since the southeast monsoon also affects large parts of Korea during summer. In general, the tritium level of water vapor over the sea is depleted in tritium due to the dilution effect with oceanic water vapor (Bolin, 1958). Seasonal variations of tritium in precipitation have been reported in other areas of the world, but with the different trends. For example, in Australian precipitation, the maximum tritium values were observed in early spring (August and September) and the minimum values were observed in March and April (Tadros et al., 2014). In Ramnicu Valcea, Romania, a significant maximum level was noted during the late spring-summer months (Duliu et al., 2018). In Hanoi, Vietnam, decreased levels were observed from June to September (Anh et al., 2018). In Fukuoka, Japan, increased values were recorded during winter and spring, whereas decreased values were obtained during summer and fall (Hayashi et al., 1999). Therefore, the seasonal variations of tritium in

precipitation seem to be affected by various geographical and meteorological factors.

The magnitude of seasonal variations was smaller at stations located in the island (St. S1–S3) and coastal regions (St. C1, C3, C4) than those located inland stations (N1–N9) (Figure 2.3–2.5), owing to more frequent incursions of marine airs. The difference between the maximum and minimum values at St. S3 (2.9–6.2 TU), which is located on Jeju Island, displays the lowest value amongst the entire sampling stations. As such, the average concentrations of tritium in precipitation from 2003 to 2011 increased with increasing distance of the sampling station from the coastline, except for station C4 (Figure 2.6). The values were less than 7 TU at the sampling stations in most of the islands and coastal areas. This geographical trend is consistent with the previously reported results in California (USA) and Australia (Harms et al., 2016; Tadros et al., 2014). Amongst the stations, station C4 showed unusually high peak in January; as this station is situated in proximity to Wolsong nuclear power plants (NPPs), we believe that the dominant northerly wind results in this unusual trend during winter.

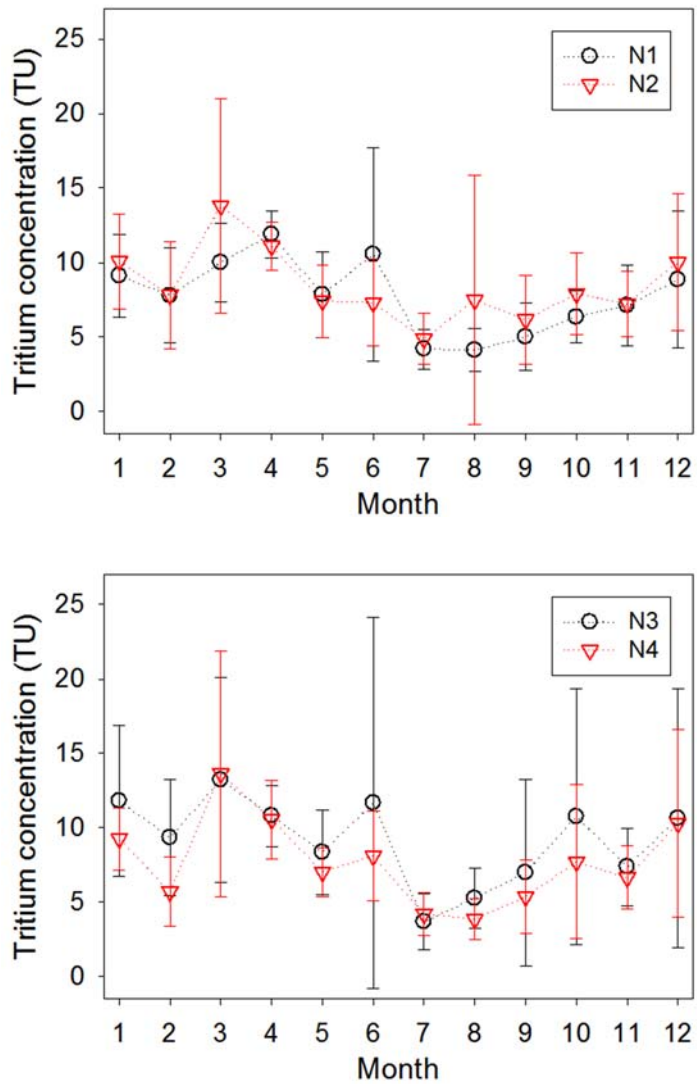

Figure 2.3. Average concentrations of tritium for each month in precipitation from 2003 to 2011 at St. N1–N4. The error bars represent the standard deviations.

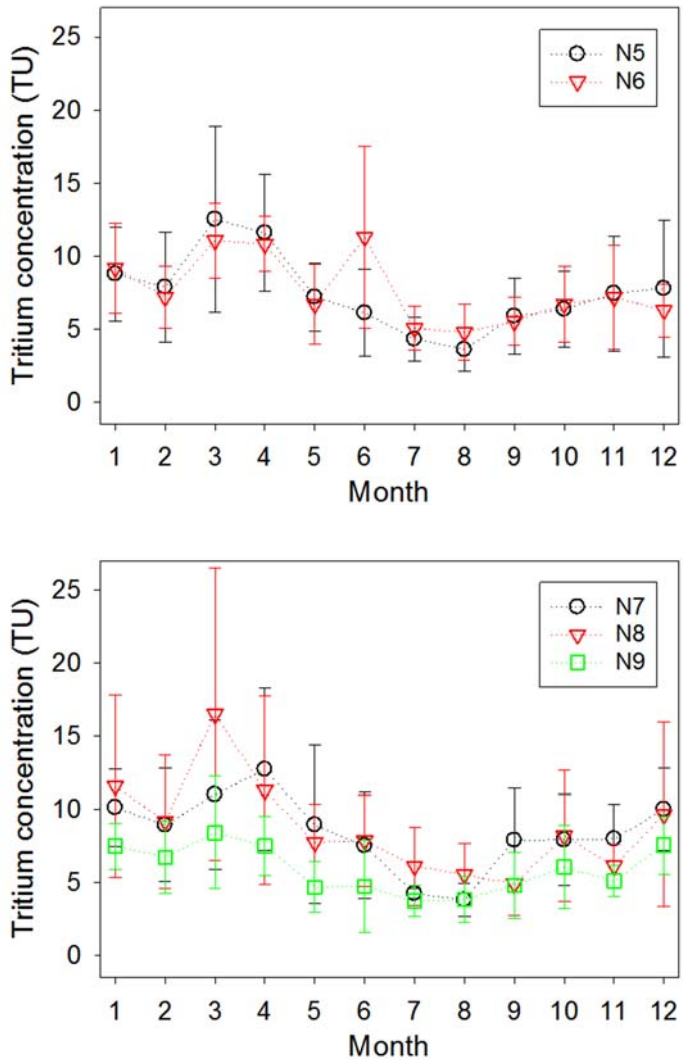

Figure 2.4. Average concentrations of tritium for each month in precipitation from 2003 to 2011 at St. N5–N9. The error bars represent the standard deviations.

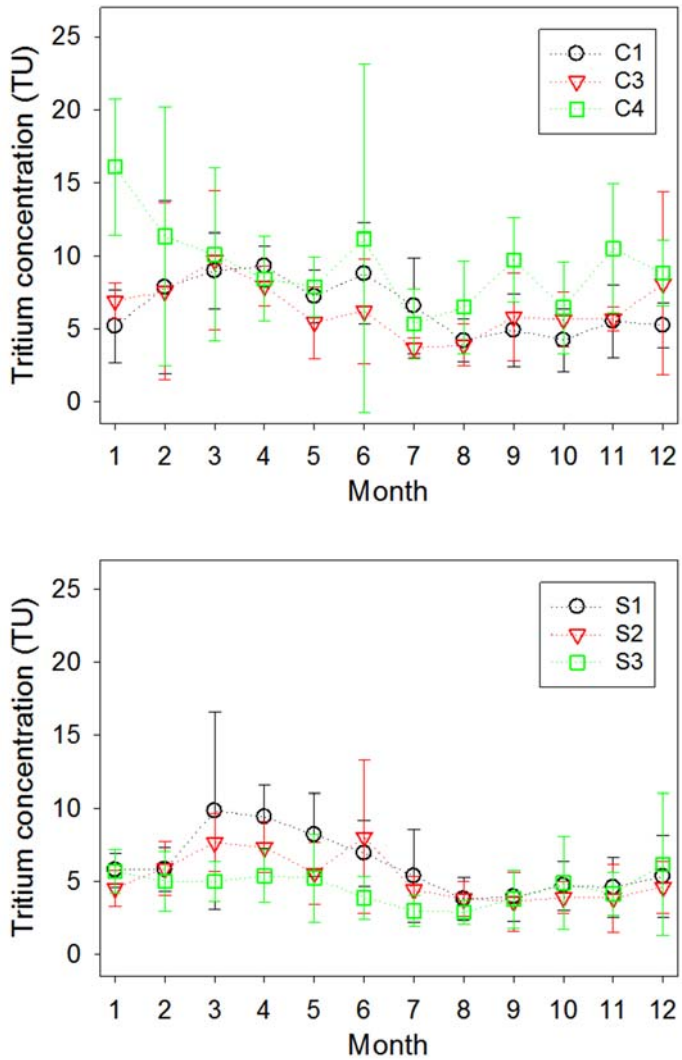

Figure 2.5. Average concentrations of tritium for each month in precipitation from 2003 to 2011 at St. C1, C3–C4 and S1–S3. The error bars represent the standard deviations.

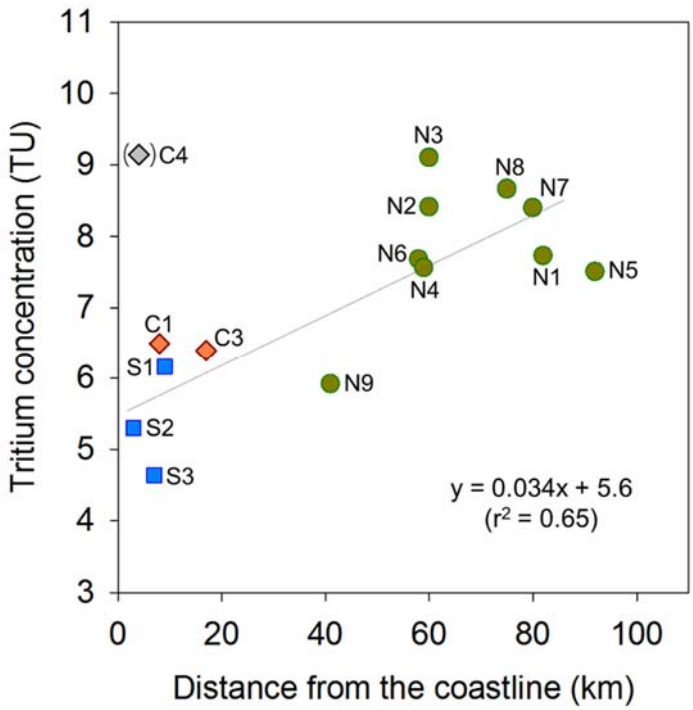

Figure 2.6. The plot of average tritium concentrations in precipitation for 15 sampling stations from 2003 to 2011 against the distance of sampling stations from the coastline in Korea. The tritium value of station C4 in parentheses is excluded when evaluating the correlation. Green circles, orange diamonds, and blue squares represent the sampling stations located inland, on the coast, and on the islands, respectively.

2.3.2. Meteorological factors controlling tritium levels in air

In order to evaluate the effect of precipitation amounts on tritium values, the correlations between tritium concentrations and precipitation amounts were examined for different regions. The monthly tritium concentration was normalized to the 12-month average. The normalized tritium values (monthly ^{3}H concentration/12-month ^{3}H concentration) were negatively correlated with the amount of precipitation (Figure 2.7– 2.12). Such a precipitation amount effect was observed in the monthly tritium data for certain inland sites in Australia (Tadros et al., 2014). However, no correlation was reported for Hanoi, Vietnam, since the rainfall during the dry season is monsoonal and is small or even rainless (Anh et al., 2018).

The negative correlations between tritium concentrations and precipitation amounts could be observed due to fractionation of hydrogen isotopes and the timing of the stratosphere-troposphere exchange during the low precipitation period. Korea is characterized by four distinct seasons and the period of monsoon. In order to eliminate this seasonal effect, the monthly tritium concentrations in precipitation during summer (June, July, and August) were used separately (Figure 2.8, 2.10, and 2.12). We still observe weak negative correlations between tritium concentrations in precipitation and the amount of precipitation for all three different group regions (inland, coast, and island) during the summer. These negative correlations could be explained by this fractionation effect. The fractionation of hydrogen-deuterium isotopes by evaporation and condensation processes has been previously reported (Craig and Gordon, 1965). In the case of tritium, it is known to be more strongly

fractionated due to its larger mass difference (Herczeg and Imboden, 1988). In general, HTO is preferentially condensed due to its lower saturation vapor pressure than H_2O (Craig and Lal, 1961) and can be concentrated in early rainout and diluted in more complete rainout. Thus, we suggest that the precipitation amount effect could be associated with various factors including isotopic fractionation, precipitation frequency, and seasonal variation.

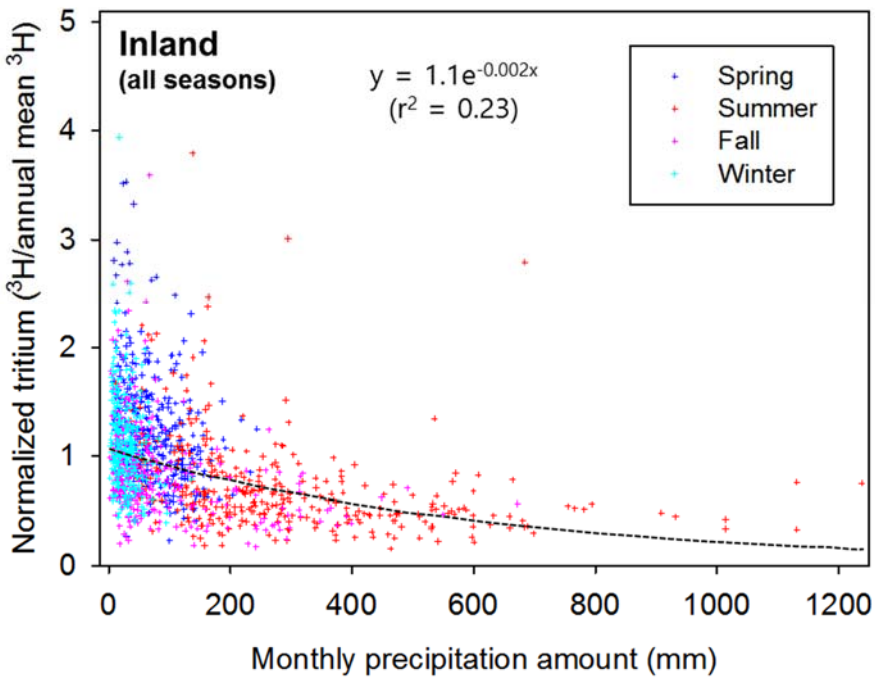

Figure 2.7. A plot between tritium (^{3}H/annual mean ^{3}H) concentrations in precipitation, normalized for annual ^{3}H, versus the monthly precipitation amounts during the four seasons at inland sampling stations.

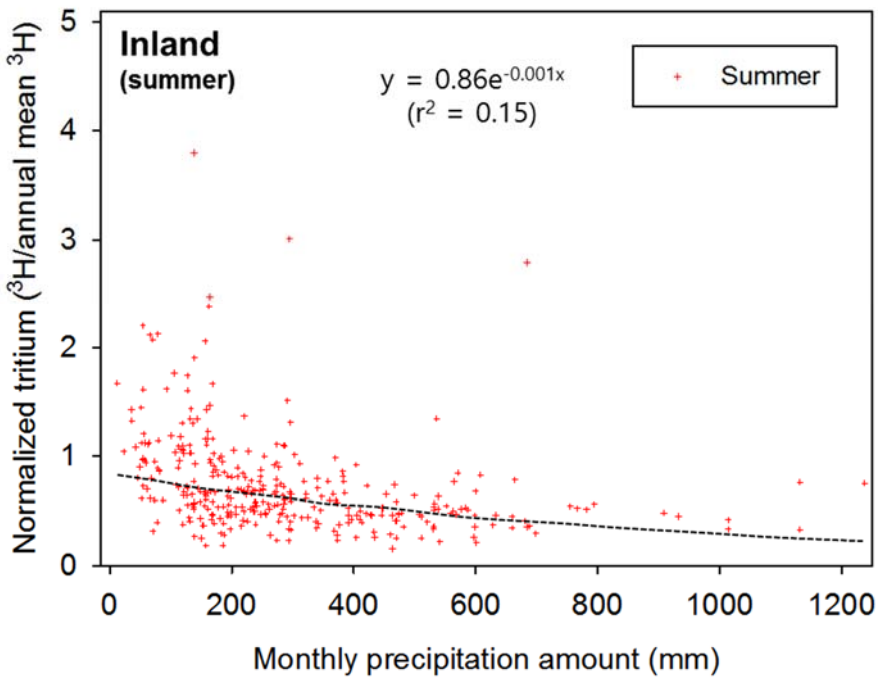

Figure 2.8. A plot between tritium (^{3}H/annual mean ^{3}H) concentrations in precipitation, normalized for annual ^{3}H, versus the monthly precipitation amounts in the summer at inland sampling stations.

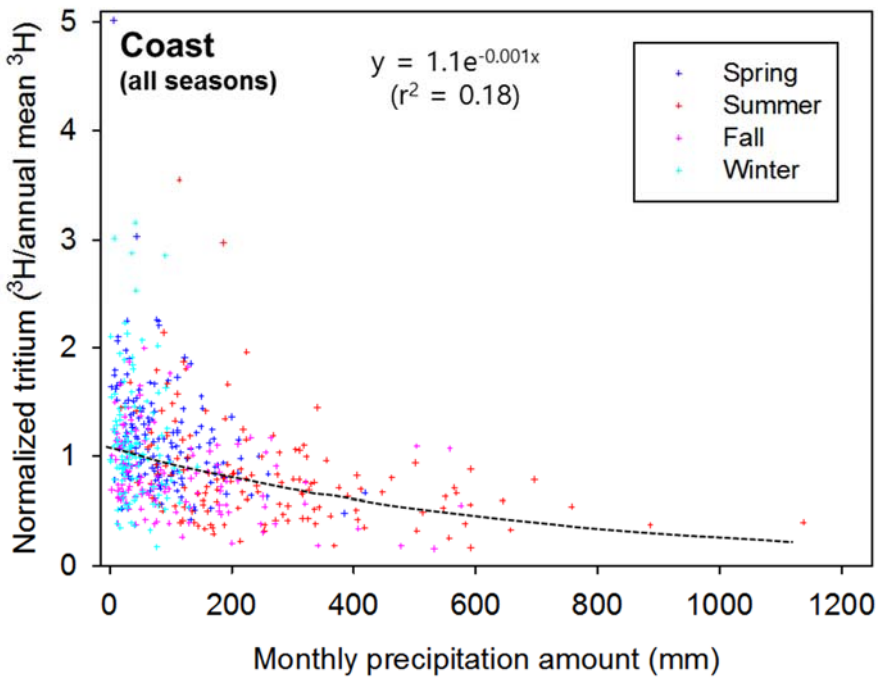

Figure 2.9. A plot between tritium (^{3}H/annual mean ^{3}H) concentrations in precipitation, normalized for annual ^{3}H, versus the monthly precipitation amounts during the four seasons at sampling stations located along the coast.

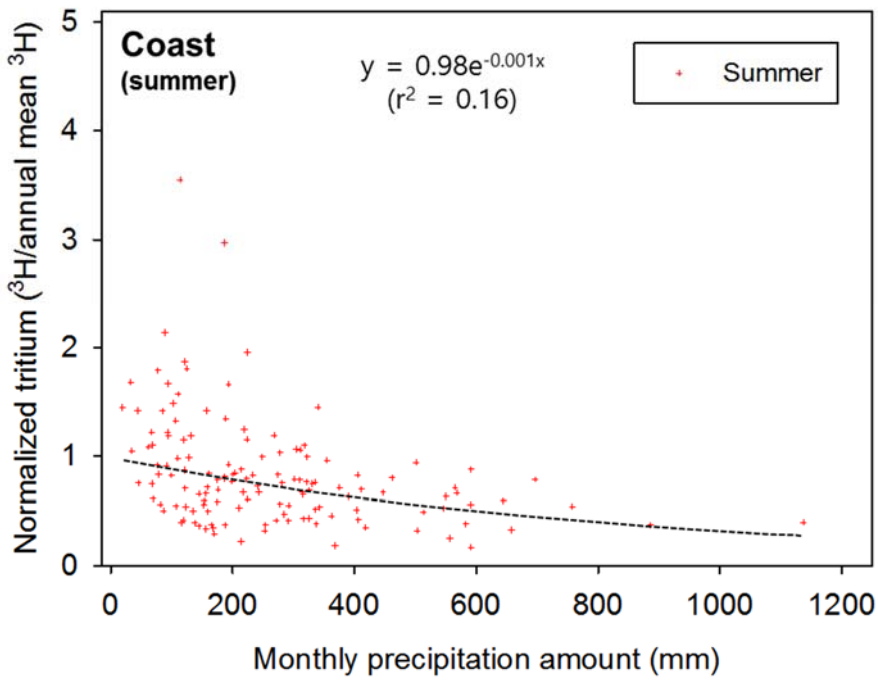

Figure 2.10. A plot between tritium (^{3}H/annual mean ^{3}H) concentrations in precipitation, normalized for annual ^{3}H, versus the monthly precipitation amounts in the summer at sampling stations located along the coast.

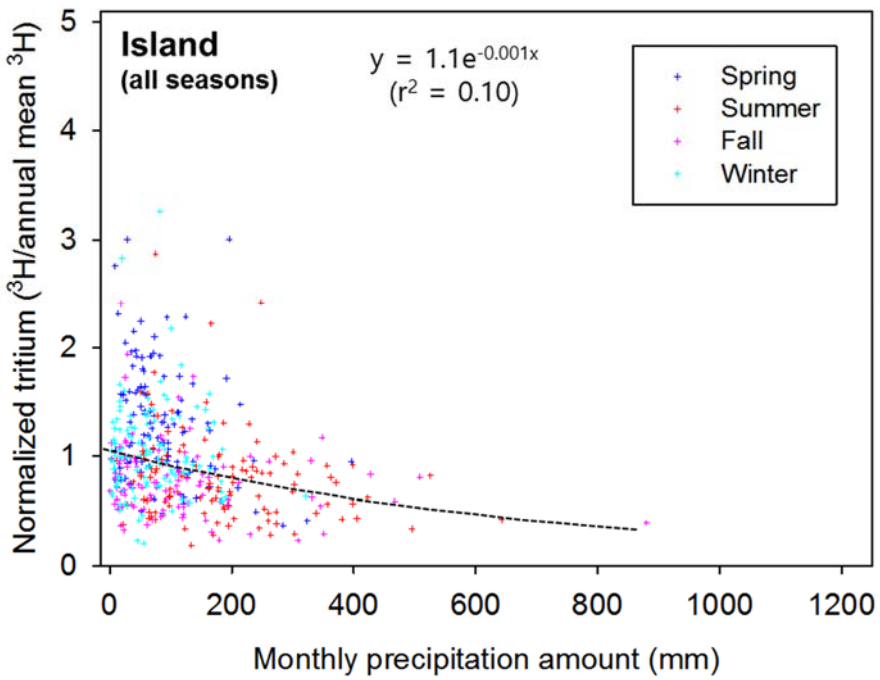

Figure 2.11. A plot between tritium (^{3}H/annual mean ^{3}H) concentrations in precipitation, normalized for annual ^{3}H, versus the monthly precipitation amounts during the four seasons at sampling stations located in the island.

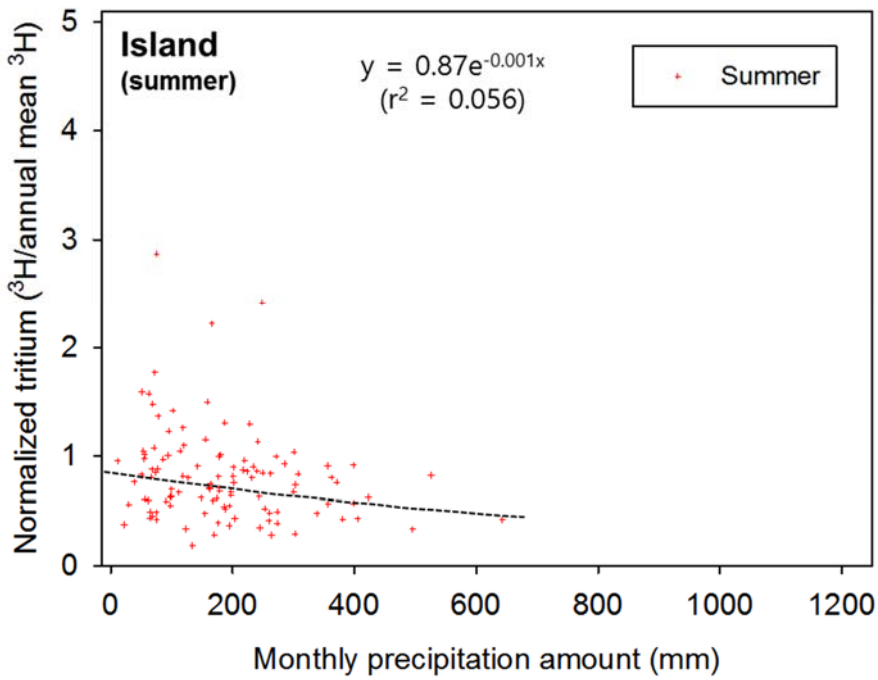

Figure 2.12. A plot between tritium (^{3}H/annual mean ^{3}H) concentrations in precipitation, normalized for annual ^{3}H, versus the monthly precipitation amounts in the summer at sampling stations located in the island.

2.3.3. Tritium levels in precipitation for different regions in East Asia

The annual mean values of tritium concentrations in Korea, normalized by precipitation amount, peaked (1385 TU) in 1963 due to the effects of global atmospheric nuclear weapons testing prior to the 1963 Partial Test Ban Treaty (PTBT) (Figure 2.13). The levels of tritium decreased rapidly from 1963 to 1968 and then gradually decreased thereafter. Although tritium concentrations decrease gradually after 1968, there were small transient increases in 1971 and 1974 due to the effects of the French and Chinese nuclear tests. Since the late 1990s, the level has maintained a constant value of less than 10 TU (Figure 2.14).

The tritium level in Korea was relatively lower than that of Ottawa and Vienna since Korea is located at a lower latitude than Ottawa and Vienna, but higher than that of Addis Ababa located in low latitude area and Melbourne in the South Hemisphere (Figure 2.15 and 2.16). Compared with other regions in Asia, the tritium level in Korea was approximately twice as high as that of Hong Kong in Southeast Asia. However, its value was half of the value observed in Shijiazhuang, China (Figure 2.17). This is because in spite of being located at a similar latitude to Korea, Shijiazhuang is comparatively less affected by the oceanic water vapor. The tritium level in Japan was slightly lower than that in Korea. Thus, dominant marine air effects can be one of the causes for the difference, considering both countries are located at a similar latitude.

The average tritium concentration in precipitation in Korea was 5.7 TU from

1998 to 2011. The tritium values were high in the order of inland (6.4 TU), coastal areas (5.6 TU), and islands (5.2 TU). In order to establish the relative concentration factors of tritium for different regions in Asia, we calculated f value, which is the ratio of tritium concentration at each station to the mean tritium concentration in the Korean coastal area. We used the Korean coastal value since the seasonal variations of tritium is small and data are abundant. The f values ranged from 0.32 to 4.3 in East Asia (Figure 2.18). Indeed, the values are high at Wulumuqi, China (f = 4.3) and Shijiazhuang, China (f = 3.5), which are higher than the f value (f = 2.9) at Ottawa station. Compared with these Chinese stations, South Asian stations, including Hong Kong (China), Bangkok (Thailand), and Diliman Quezon City (Philippines) showed lower values (f = 0.32 – 0.46) (Figure 2.19). Thus, the f ratios can be established for other regions in the world, including other regions in Asia, in order to use more accurate initial tritium values in hydrology. If the long-term history of tritium in precipitation is necessary, our long-term trend can be also used as an index.

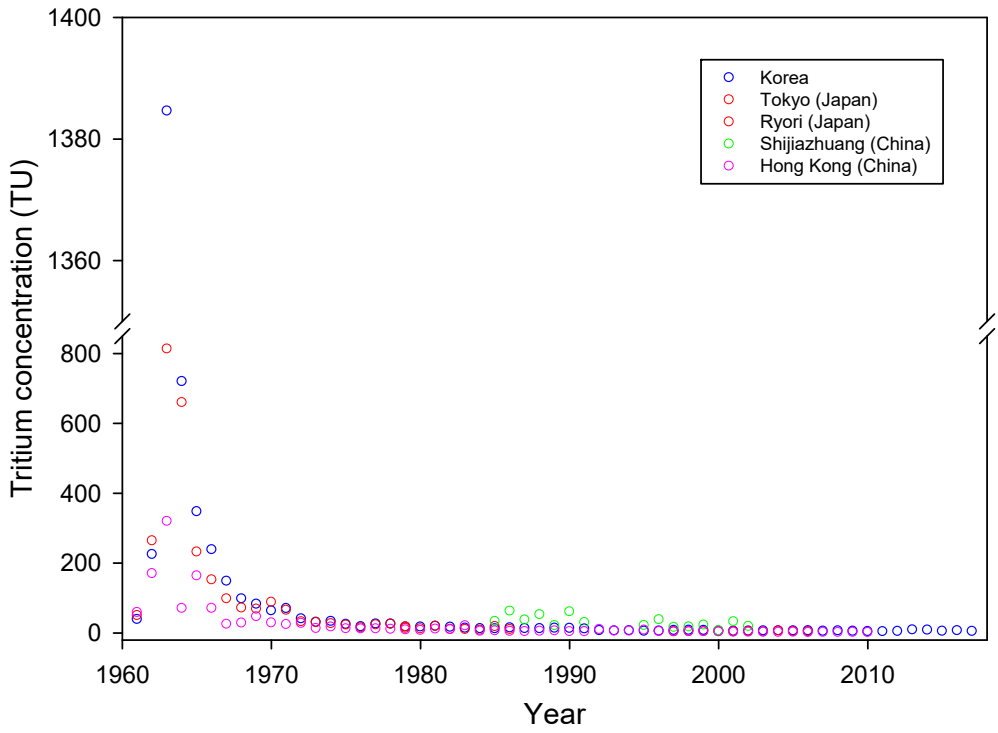

Figure 2.13. Long-term variations of the weighted mean annual tritium concentrations in precipitation in Korea from 1961 to 2016, in comparison with other stations in Asia.

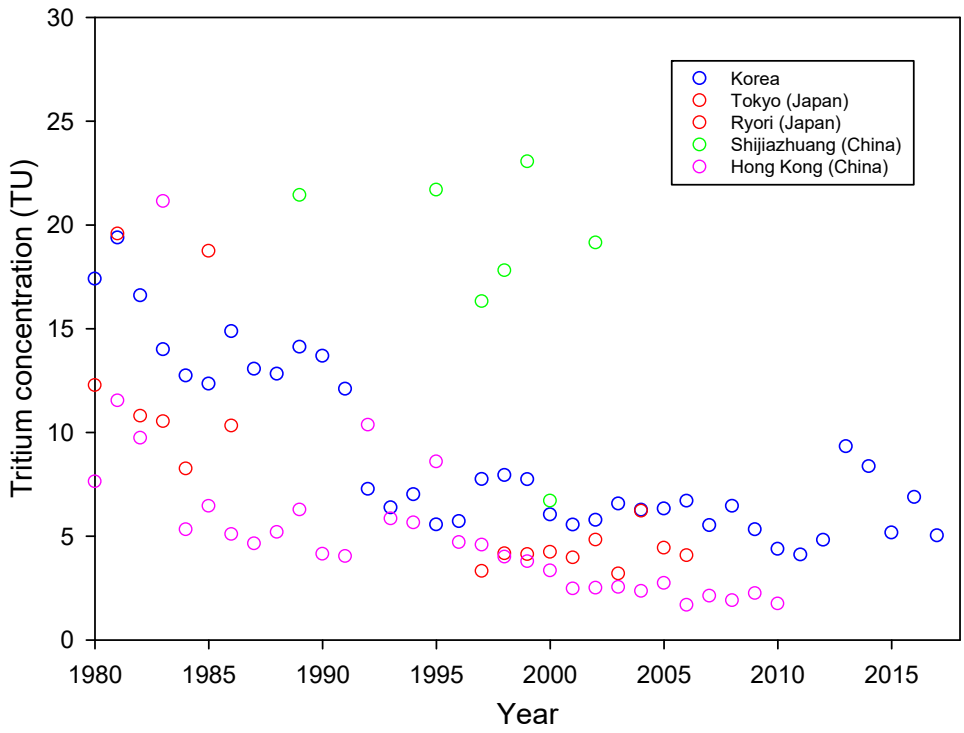

Figure 2.14. Long-term variations of the weighted mean annual tritium concentrations in precipitation in Korea from 1980 to 2016, in comparison with other stations in Asia.

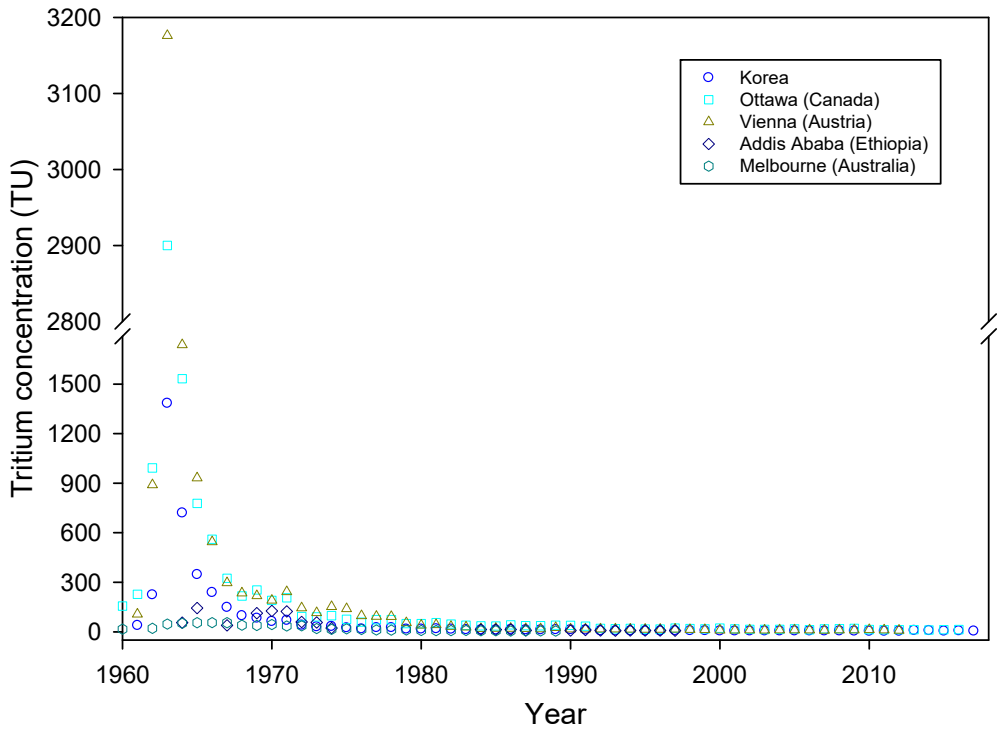

Figure 2.15. Long-term variations of the weighted mean annual tritium concentrations in precipitation in Korea from 1961 to 2017, in comparison with other stations in the world.

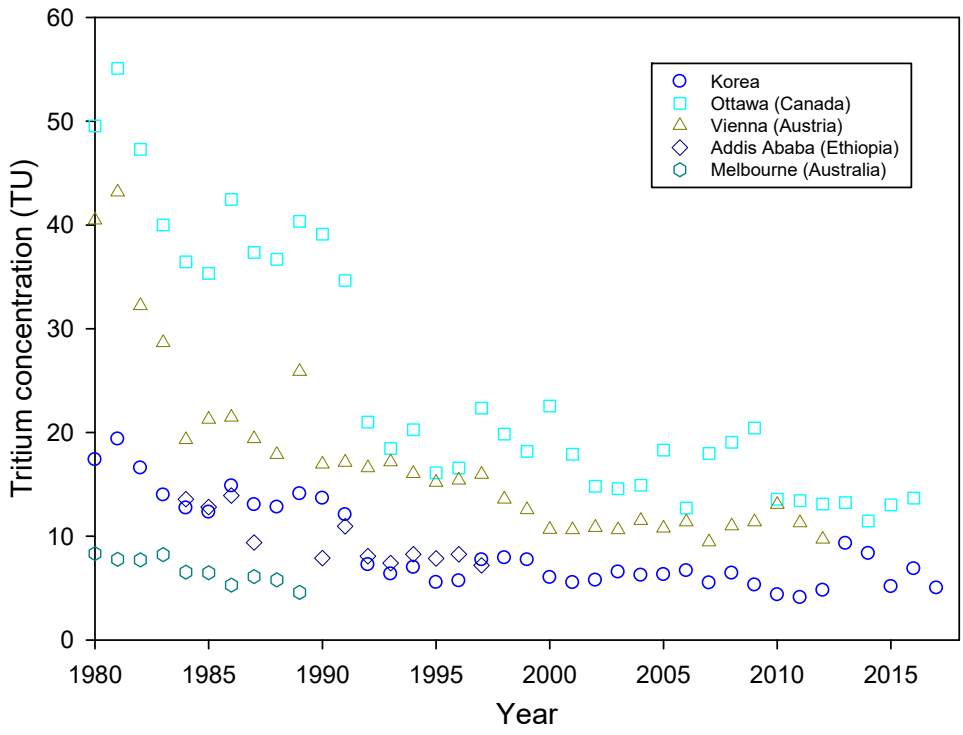

Figure 2.16. Long-term variations of the weighted mean annual tritium concentrations in precipitation in Korea from 1980 to 2017, in comparison with other stations in the world.

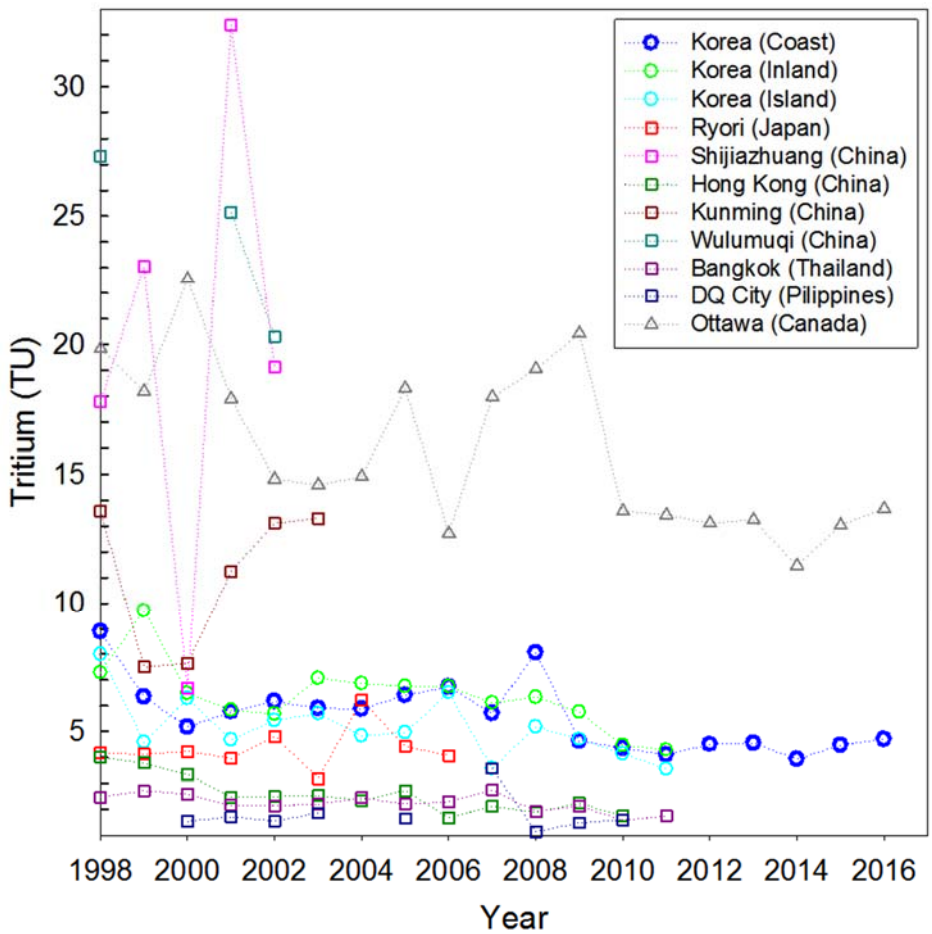

Figure 2.17. Precipitation amount-weighted mean annual tritium concentrations in precipitation at different stations throughout East Asia and station at Ottawa, Canada, from 1998 to 2016.

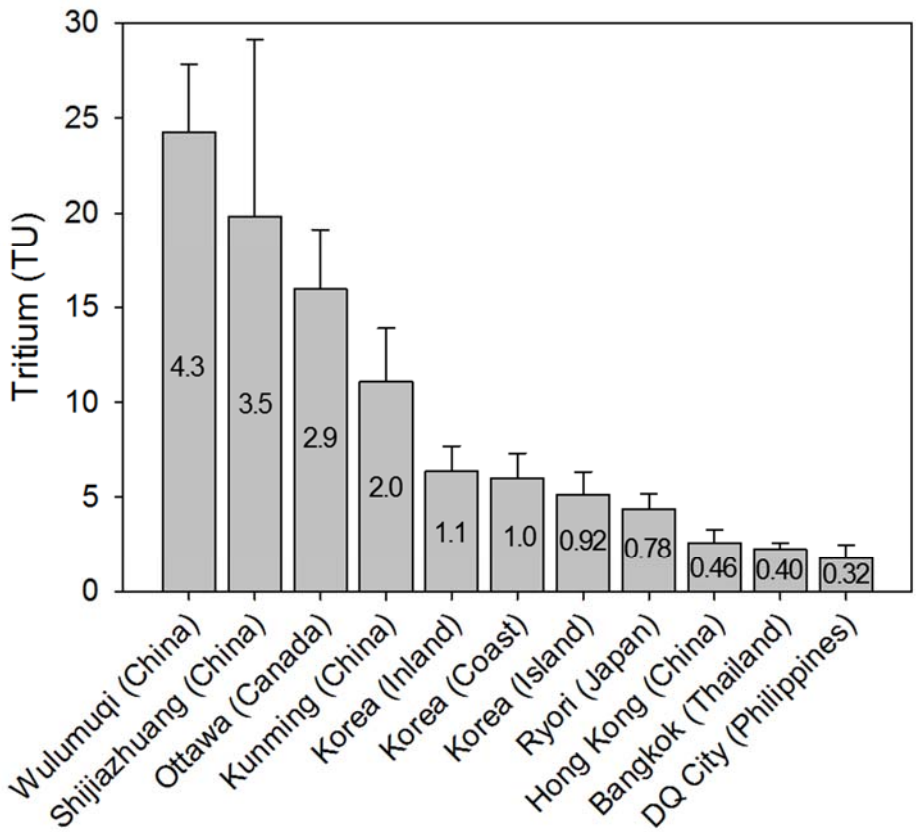

Figure 2.18. The mean values of annual tritium concentrations over the period for each sampling station. The ratio (f values) of tritium concentration at each station to the mean tritium concentration in the Korean coastal area is shown in the bar.

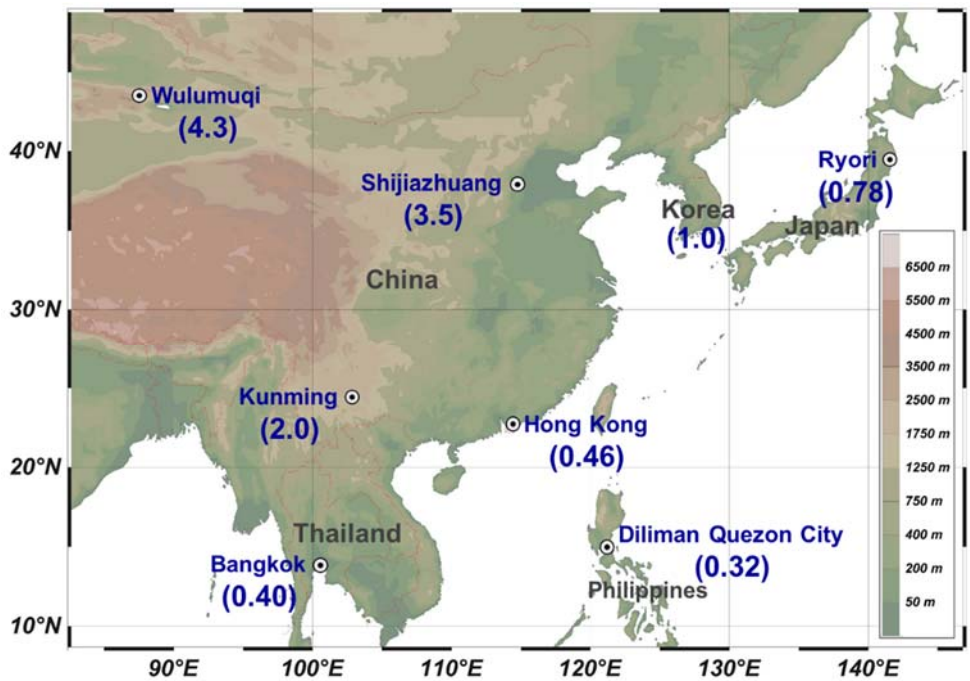

Figure 2.19. The ratio (f values) of tritium concentration at each station throughout East Asia to the mean tritium concentration in the Korean coastal area.

2.4. Conclusions

The temporal and spatial variations of tritium in precipitation were investigated at 16 stations in Korea. The seasonal variations of tritium concentration in precipitation showed the maximum value in spring due to the stratosphere–troposphere air exchange and minimum values in summer due to dominant oceanic air inflows related to the monsoon. The magnitude of seasonal variation in tritium concentrations varied depending on the contribution of marine air which has low tritium concentrations. Thus, the seasonal variations were smaller for coastal and island stations. As such, the tritium concentrations in precipitation increased with the distance from the coastline to the land due to influence of marine air. The tritium concentrations in precipitation decreased as the amount of precipitation increased, perhaps due to the fractionation of tritium relative to hydrogen in the course of rainout as well as difference in the origin of rain clouds. The concentrations of tritium in precipitation in Asia showed an order of magnitude differences, depending on geographical and meteorological characteristics of the region. Thus, our results of tritium in precipitation in Korea will serve as an important index of tritium levels in precipitation in understanding water cycles and meteorological characteristics in Asia.

3. Large seasonal variations in aerosol precipitation rates revealed using the cosmogenic ^{7}Be tracer

3.1. Introduction

Beryllium-7 is a relatively short-lived (half-life: 53.3 days) naturally occurring cosmogenic radionuclide produced by the spallation processes of light atmospheric nuclei such as carbon, nitrogen, and oxygen, when they absorb the protons and even neutrons of the primary component of cosmic radiation (Masarik and Beer, 1999; Papastefanou and Ioannidou, 1995; Rindi and Charalambus, 1967). Approximately 70% of ^{7}Be is produced in the stratosphere (Kathren, 1984) and the remaining 30% is produced in the high troposphere. The concentration of ^{7}Be is the maximum at a height of 15-20 km, and it exponentially decreases with altitude, toward the Earth's surface. After production, ^{7}Be is rapidly adsorbed onto aerosol particles, primarily submicron-size (from 0.07 to 2 μm diameter), which are major reservoir of pollutants in the atmosphere (Papastefanou and Ioannidou, 1995) and removed to the Earth's surface by dry and wet fallout.

The concentrations of ^{7}Be are affected by various factors depending on locations, such as the air exchange between the stratosphere and the troposphere (Feely et al., 1989), scavenging by precipitation (Baskaran et al., 1993; Benitez-Nelson and Buesseler, 1999; Wallbrink and Murray, 1994), and horizontal transport (Rahn, 1981). Thus, ^{7}Be has been utilized to trace the intrusion of stratospheric air in the troposphere (Graustein and Turekian, 1996) and to trace the deposition velocity of aerosols (Dueñas et al., 2005). ^{7}Be also has been utilized together with radon daughter, ^{210}Pb, or cosmogenic ^{35}S, to understand aerosol transports and

material cycling in the atmosphere (Brost et al., 1991; Cho et al., 2011; Kim et al., 1999; Kim et al., 2000b; Koch et al., 1996; Lee et al., 2004).

Particulate matter (PM) is a key air pollutant for air quality (Li et al., 2003; Ostro et al., 2015; Samoli et al., 2013) and climate change (Lohmann and Feichter, 2005; Ramanathan and Feng, 2009). Natural PM is affected significantly by mineral dust transport from the deserts (Zhang et al., 2003). In addition, there is an increasing amount of anthropogenic PM sources, such as factories, biomass burning, refineries, power plants, construction activities, and fossil fuel burning (Parekh et al., 2001). Extensive modeling studies have been conducted to locate the pollution sources and predict PM10 and PM2.5 occurrences for different locations (Jerrett et al., 2004; Wang et al., 2013). However, there are still large discrepancies between modeling results and observations (Chatani et al., 2011; Huneeus et al., 2012; In and Kim, 2010; Koo et al., 2008; Shimadera et al., 2009; Wang et al., 2010) due to unknown sources and removal processes.

Thus, in this study, we compiled ^{7}Be data for aerosols and precipitation collected over 20 years in Daejeon, Korea, in order to more accurately determine the long-term seasonal variations of ^{7}Be and to calculate the depositional velocities of fine aerosols, which are extremely complicated and poorly understood, using ^{7}Be as a tracer (McNeary and Baskaran, 2003; Papastefanou and Ioannidou, 1991; Todd et al., 1989; Turekian et al., 1983). ^{7}Be is known to be produced only in the atmosphere and has a high affinity to fine particles upon production. Thus, in this study, we hypothesized that such a long-term data set of ^{7}Be tracer is unique and powerful for understanding the removal efficiencies of fine aerosols in this region.

3.2. Materials and methods

3.2.1. Study area

The sampling station is located in Daejeon in the province of Chungcheongnam-do, located in the middle of South Korea in Northeast Asia. The monthly average temperature of this city ranges from -6 to 29℃, with an annual average value of 13℃. The monthly precipitation amount ranges from 2 to 782 mm, with an annual precipitation amount of 1360 mm. The sampling station is about 5 m above the ground at the Korea Institute of Nuclear Safety in Daejeon (36°22'26"N; 127°22'10"W).

3.2.2. Data acquisition

Basic data for ^{7}Be activity concentrations in surface air and precipitation are available in the annual reports published by the Korea Institute of Nuclear Safety (KINS) (KINS, 1998-2017). The concentrations of ^{7}Be as well as other natural and artificial radionuclides in the surface air and precipitation were obtained from the nationwide monitoring program of KINS over 20 years. Meteorological data such as precipitation amount, relative humidity, and temperature were obtained from the Korea Meteorological Administration (KMA) database (KMA, 2018). The meteorological data and PM10 data were obtained from the locations close to the ^{7}Be sampling station (< 500 m distance) (NIER, 1999-2014).

3.2.3. Analytical methods

The methods for sampling and analysis of ^{7}Be in aerosol and precipitation samples are described briefly. The aerosol samples were collected monthly from 1998 to 2017 using a high-volume air sampler (HVP-35000AFC/230) with a cellulose filter (Whatman, grade 41, 20.3 × 25.4 cm). This filter is known to have a collection efficiency of 99.9% or more for particles as small as 0.3 μm (Pszenny et al., 1993). The average air-flow rate of the air sampler was ~0.7 m^3 min^{-1}, and the filter was changed every two days to prevent clogging. The filters collected for a month were combined and combusted at about 450℃ in the electric furnace. Each combusted ash sample was filled into a cylindrical vial with the geometry of Ø4.8 × 4 cm^3. The activity of ^{7}Be was measured using a high purity germanium (HPGe) detector with a relative efficiency of 30%. The detection efficiency of the detector was calibrated with different sample heights from 0.2 to 5.0 cm using a commercial standard gamma source certified by the National Institute of Standards and Technology, USA. The wet precipitation samples were collected each month in a container that opens only when it is raining, with a surface area of 1.5 m^2. After the sample was moved to the laboratory, the sample was evaporated and completely dried. The other analytical procedure was the same as the procedure of the aerosol samples described above.

3.3. Results and Discussion

3.3.1. Factors controlling ^{7}Be activity in the surface air

The monthly and yearly variation in ^{7}Be in the surface air over 1998–2017 associated with the 11-year solar cycle was examined (Figure 3.1 and 3.2). Although the highest level of annual ^{7}Be concentrations were shown in 2008 and 2009 when the sunspot number was at a minimum (Figure 3.2), the correlation between both components was not significant (r^2=0.10). This trend suggests that the concentrations of ^{7}Be in the surface air were mainly influenced by various meteorological factors and removal processes rather than by production rates. If the effect of the solar cycle is examined for each month from 1998 to 2017, the activities of ^{7}Be and the annual average sunspot number showed the most significant negative correlation (r^2=0.31) in November (Figure 3.3), while the correlation coefficients in the other months were not meaningful with the highest value in April (r^2=0.12). Previous studies in other regions also showed different results for the correlations between ^{7}Be concentrations and sunspot numbers: no significant correlations (r=-0.024) in Granada, Spain (Piñero García et al., 2012) and good correlations in Kuwait City and Palermo, Italy (r=-0.72). In general, the correlations were more significant in the region where the fluctuation in meteorological influences are relatively small (Al-Azmi et al., 2001; Cannizzaro et al., 2004). In this study, we do not consider the influence of the solar cycle in analyzing the factors controlling the variations of ^{7}Be in the surface air or for tracing deposition velocities since the solar cycle is only important for a long-term variation.

The activity of ^{7}Be was in the range from 1.2 to 7.7 mBq m^{-3}, with an average

of 4.1 mBq m^{-3}, from 1998 to 2017 (Figure 3.4 and 3.5). This value is comparable to the activity of ^{7}Be in ground-level air at Granda (Spain) (Azahra et al., 2003), Palermo (Italy) (Cannizzaro et al., 2004), and Tokyo (Japan) (Yoshimori, 2005) reported in other studies. The monthly average activity of ^{7}Be in the surface air showed distinct seasonal variations, with a relative standard deviation (RSD) of 25%. The ^{7}Be level was relatively higher in spring but lower in summer. The higher activities in spring have been generally explained by the increased rate of the vertical air exchange between the stratosphere and the troposphere due to the thinning of the tropopause folding (Feely et al., 1989).

The wet depositional fluxes of ^{7}Be were calculated based on measured activities, precipitation amounts, and sampling periods. The annual fluxes of ^{7}Be ranged from 270 to 1148 Bq m^{-2} y^{-1} (average: 670 Bq m^{-2} y^{-1}, n=20; sampling period: 1998-2017), with monthly depositional fluxes varying from 0.01 to 318 Bq m^{-2} $month^{-1}$ (average: 56.3 Bq m^{-2} $month^{-1}$, n=238) (Figure 3.6 and 3.7). These values are comparable to the results measured in the city of Nantes, France (Laguionie et al., 2014) and are relatively lower than the results of the bulk deposition flux of ^{7}Be of 880–1780 Bq m^{-2} y^{-1} observed in Tsukuba and Osaka (970–1750 Bq m^{-2} y^{-1}), Japan (Igarashi et al., 1998; Megumi et al., 2000). The seasonal variation of the wet depositional fluxes of ^{7}Be agrees with that of precipitation (Figure 3.6 and 3.7).

The monthly ^{7}Be activities in the surface air decreased as the precipitation amounts (r^2=0.34) (Figure 3.8) and the number of days with precipitation (r^2=0.40) increased. The monthly depositional fluxes of ^{7}Be showed a positive correlation (r^2=0.50) against the precipitation amount (Figure 3.9). In addition, the monthly ^{7}Be

activities were significantly correlated with the relative humidity (r^2=0.43) in the surface air (Figure 3.10). These correlations suggest that the precipitation plays a major role on the depositional flux of ^{7}Be in the surface air.

The ^{7}Be activities also exhibited a positive correlation (r^2=0.32) with PM10 (Figure 3.11). In general, ^{7}Be is rapidly adsorbed onto fine aerosol particles and then participate in the formation and growth of the accumulation mode aerosols (0.07-2 μm diameter) (Papastefanou and Ioannidou, 1995). Thus, ^{7}Be behavior in the air is similar to that of other pollutants, transformed from gases to larger particles, which are settled either by wet or dry deposition (Ioannidou, 2011; Pan et al., 2011; Yang, 2002). Thus, the relatively good correlation between the concentrations of ^{7}Be and PM10 suggests that their concentrations are controlled mainly by the same washout effect, while the scatters could be controlled by different source inputs. Based on these facts, in this study, we use ^{7}Be as a tracer of fine aerosols.

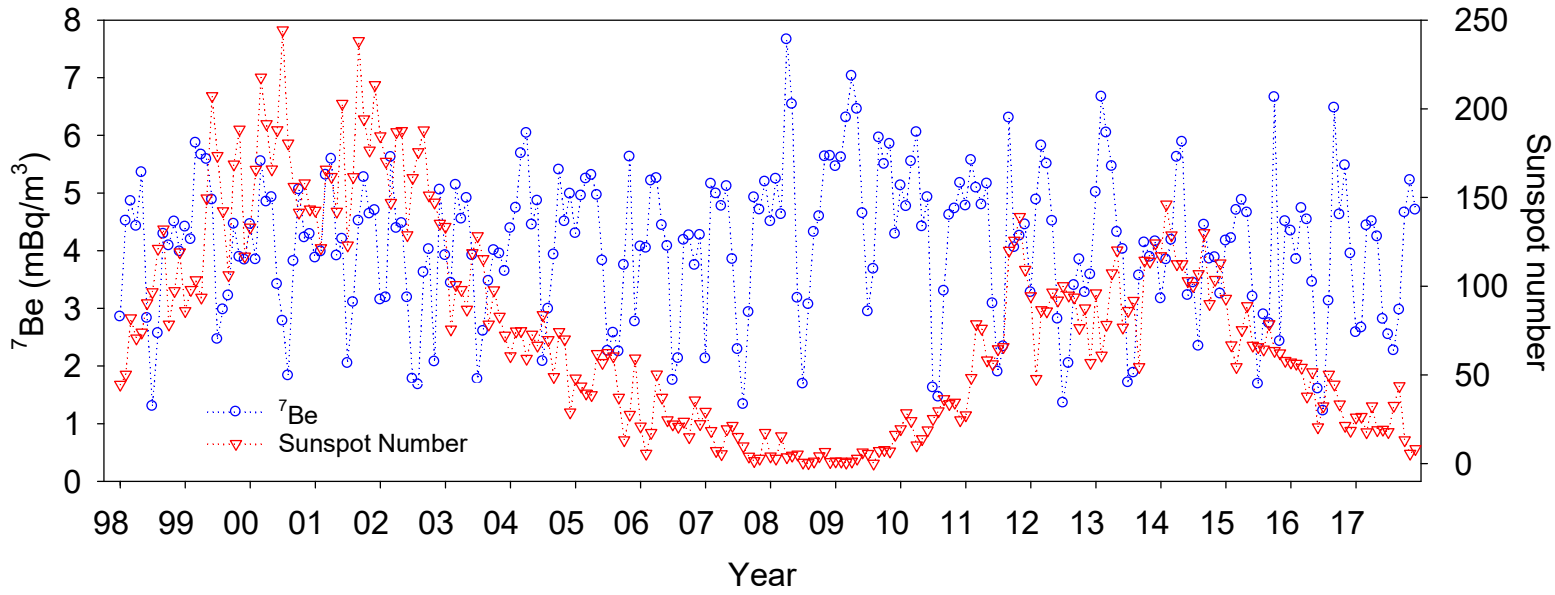

Figure 3.1. Monthly concentrations of ^{7}Be in surface air and sunspot number from 1998 to 2017.

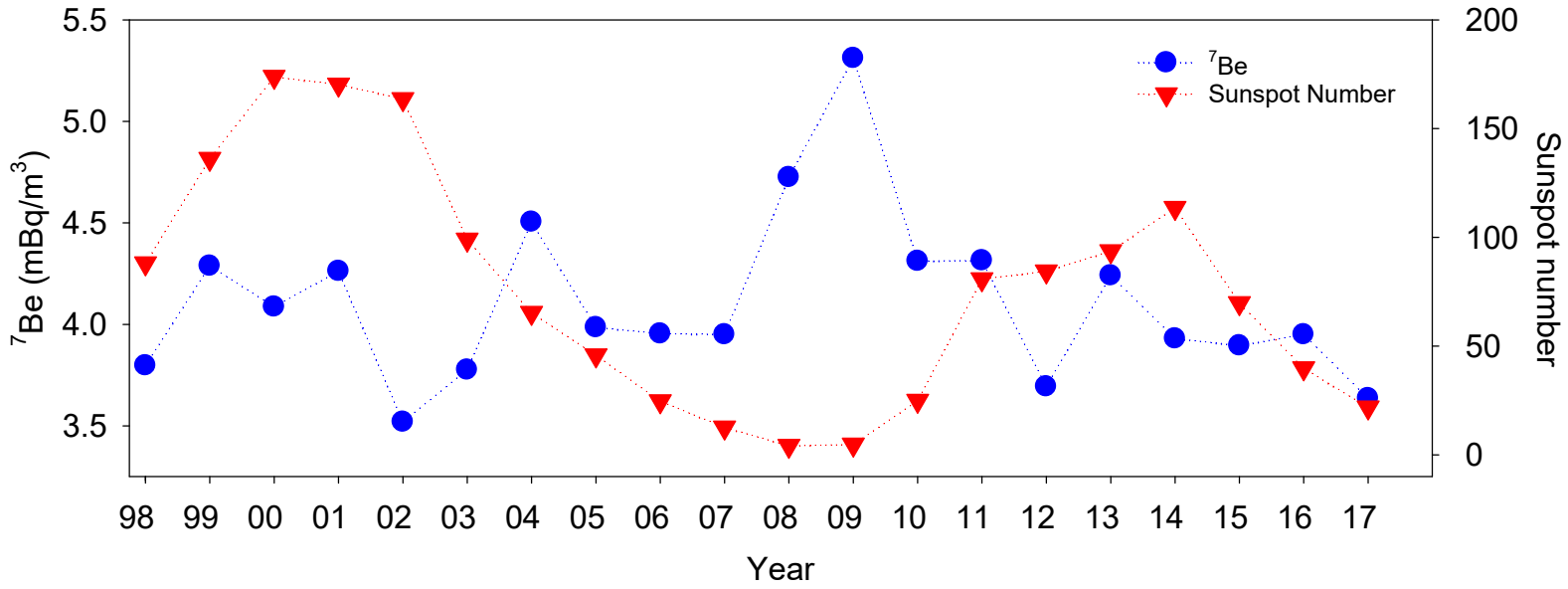

Figure 3.2. Annual average concentrations of ^{7}Be in surface air and sunspot number from 1998 to 2017.

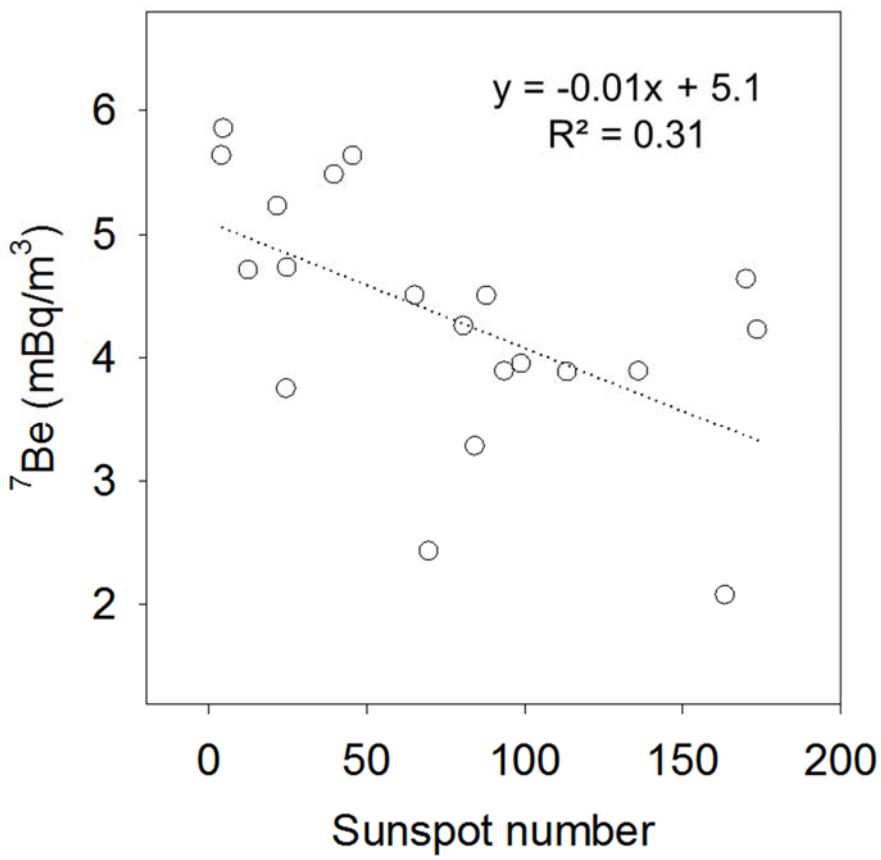

Figure 3.3. Plots of ^{7}Be activities in the surface air collected in November against the sunspot number for the period from 1998 to 2017.

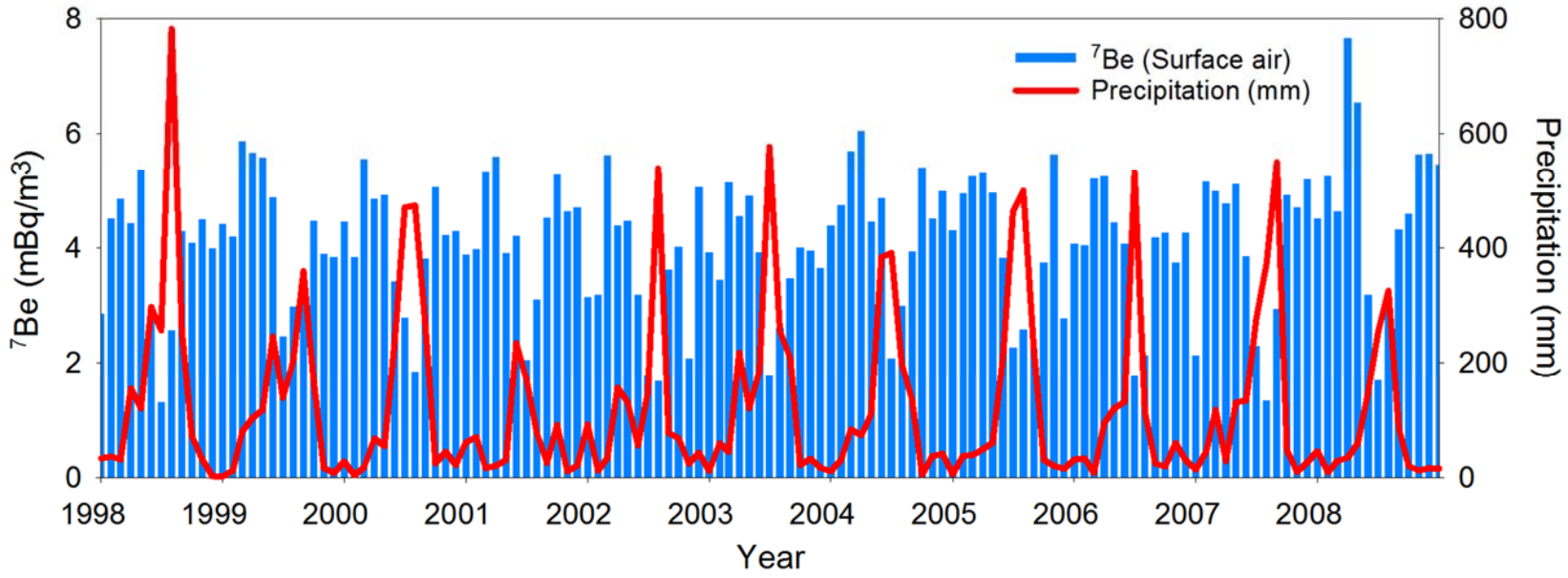

Figure 3.4. ^{7}Be concentrations in surface air and precipitation amount from 1998 to 2008.

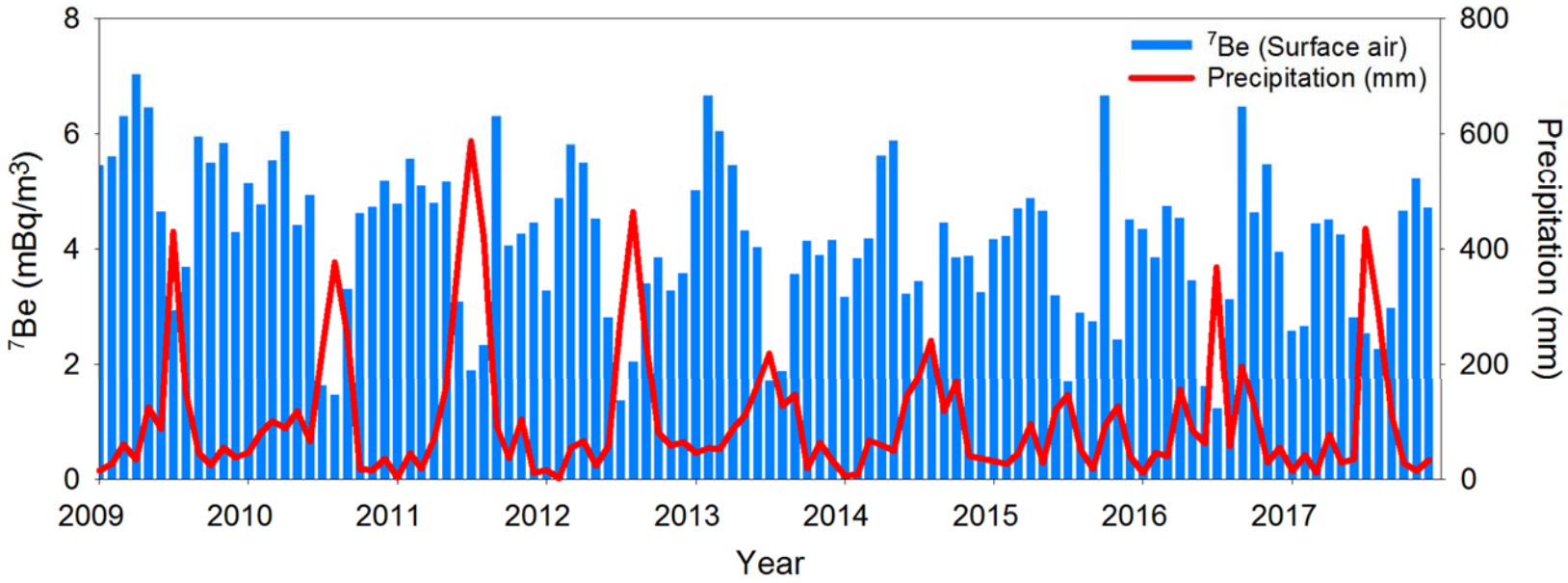

Figure 3.5. ^{7}Be concentrations in surface air and precipitation amount from 2009 to 2017.

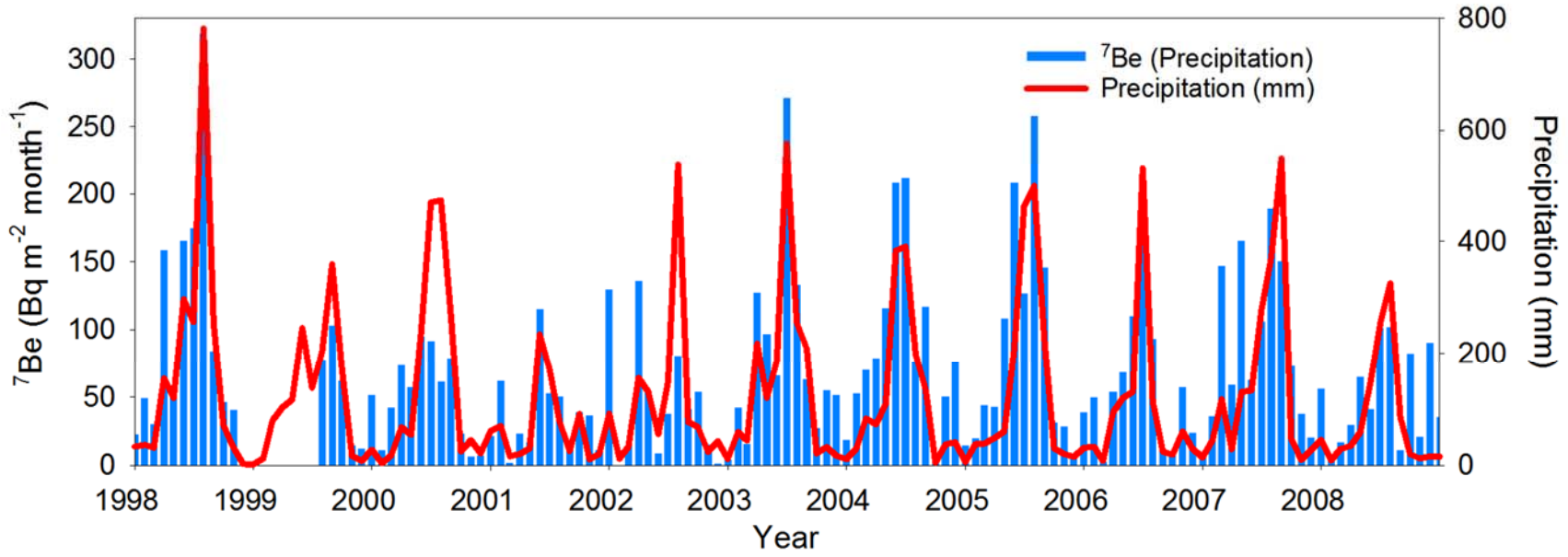

Figure 3.6. Wet depositional fluxes of ^{7}Be and precipitation amount from 1998 to 2008.

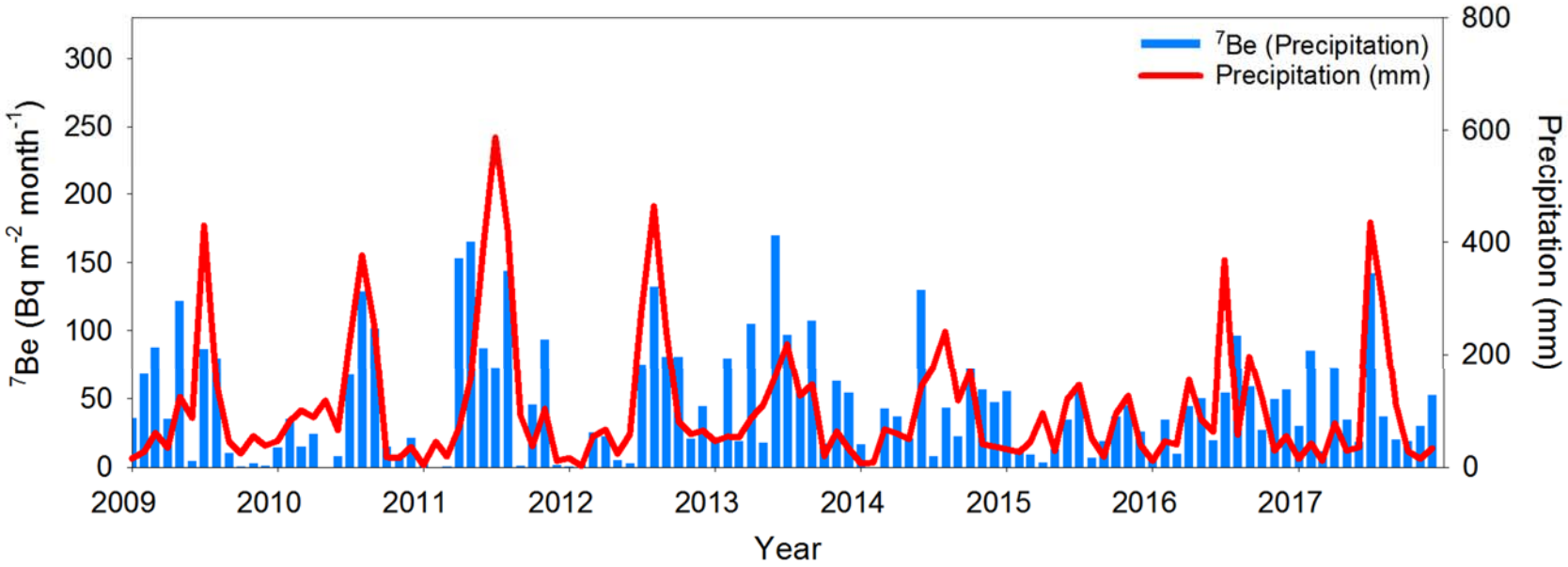

Figure 3.7. Wet depositional fluxes of ^{7}Be and precipitation amount from 2009 to 2017.

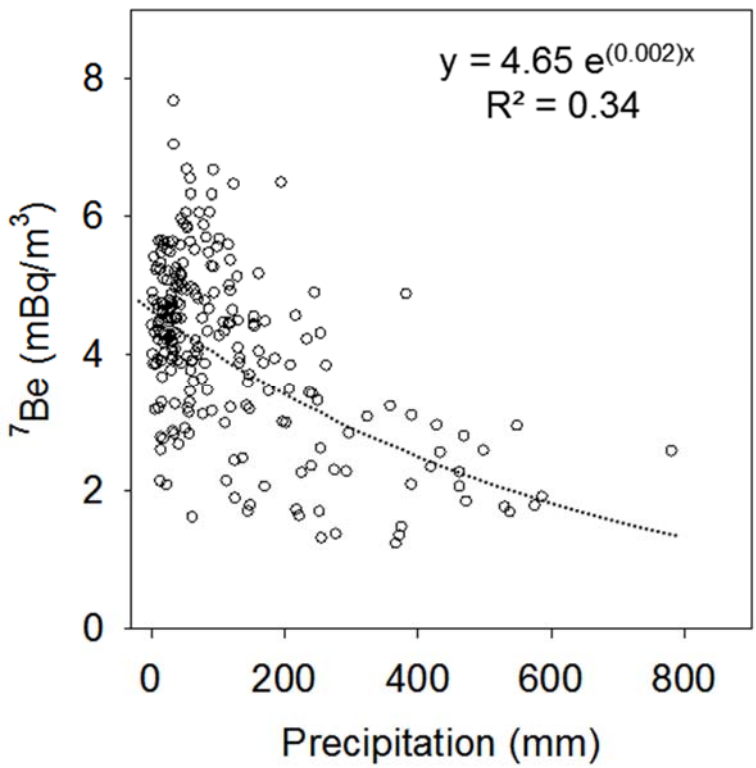

Figure 3.8. Plots of monthly activities of ^{7}Be in the surface air against the monthly precipitation amounts from 1998 to 2017.

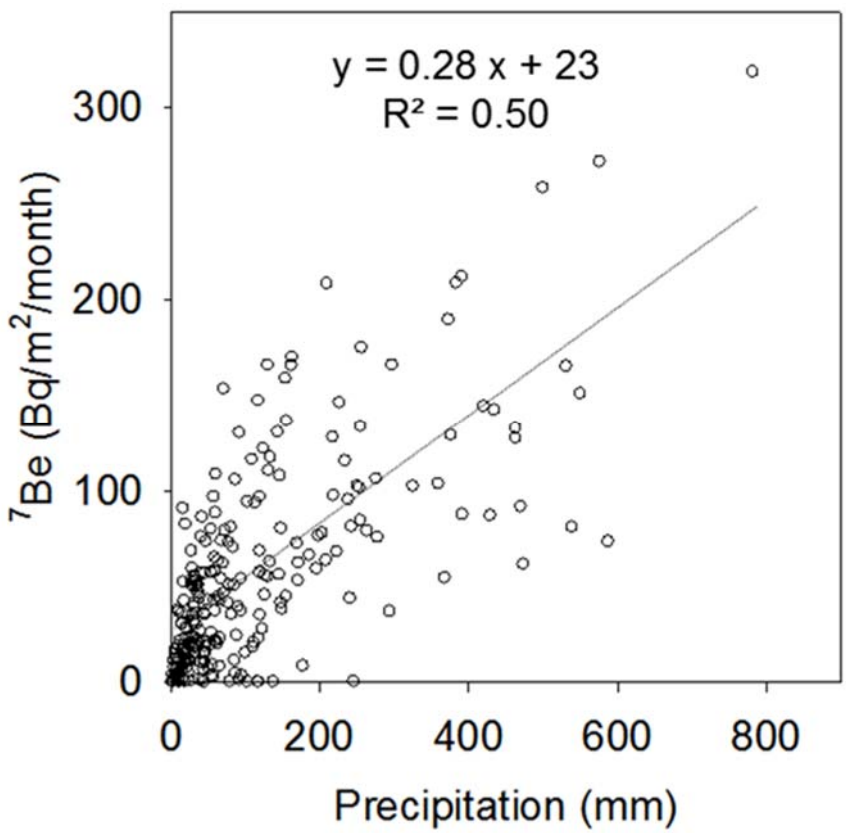

Figure 3.9. Plot of monthly wet depositional fluxes of ^{7}Be against precipitation amounts from 1998 to 2017.

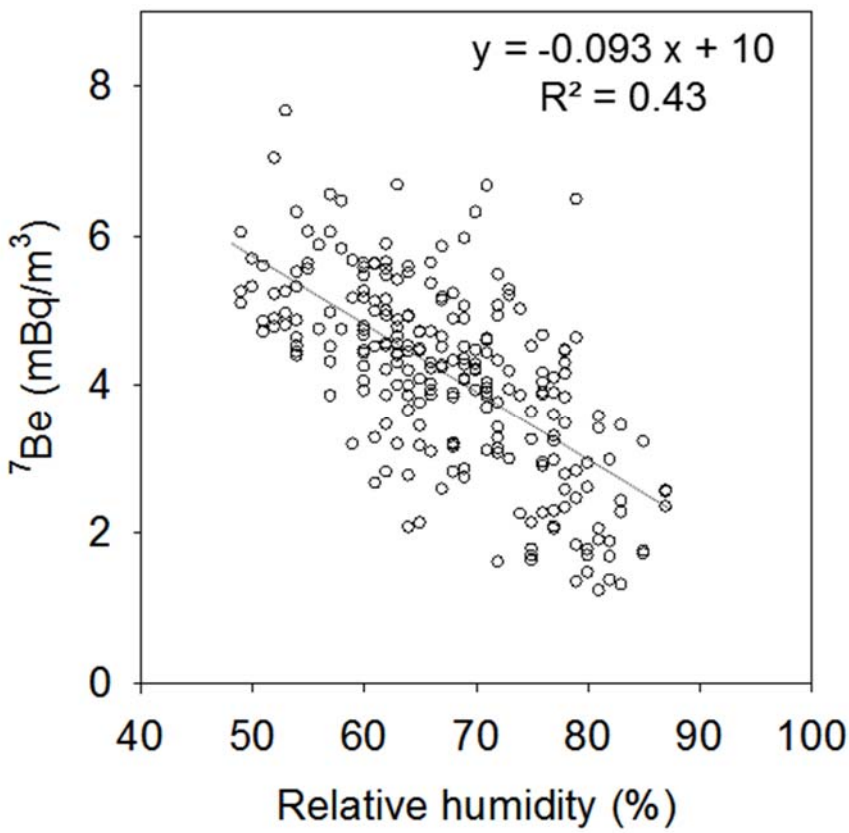

Figure 3.10. Plots of monthly activities of ^{7}Be in the surface air against the relative humidity from 1998 to 2017.

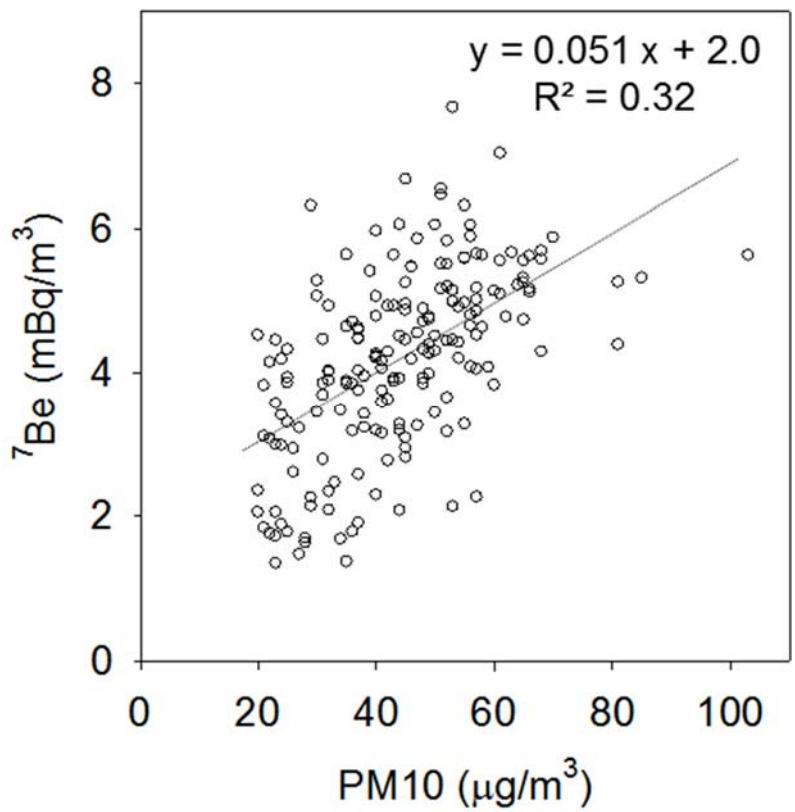

Figure 3.11. Plots of monthly activities of ^{7}Be in the surface air against the PM10 concentrations from 1999 to 2014.

3.3.2. Removal efficiency of fine aerosols

The concentration of fine aerosols (PM10) in the atmosphere is controlled by various factors such as source inputs, meteorological factors (wind speed, wind direction, and atmosphere pressure), and removal processes (dry and wet precipitation). Many previous studies have used meteorological fields and source regions, without the consideration of deposition, in order to differentiate the origins of PM10 between the external and internal sources in Seoul, Korea (Lee et al., 2011). More recent modeling approaches include the washout effect of summertime precipitation on surface air pollutants including PM10 in Korea (Yoo et al., 2014). PM10 is found to be very sensitive to precipitation particularly during the first 2 h (Yoo et al., 2014). However, the quantity of PM10 removal over different seasons in association with precipitation amounts has still been poorly understood. Most parameterization schemes for wet deposition processes, precipitation, cloud, and wind used in models are highly simplified and their performance is uncertain. Therefore, ^{7}Be tracer can provide particularly valuable information on quantitative estimations such as depositional fluxes and deposition velocities of PM10. In addition, our long-term monitoring results of ^{7}Be can reduce uncertainties associated with natural variations.

Previous studies showed that the removal of fine aerosols and ^{7}Be by dry deposition contributes to less than 10% of the total removal (Ioannidou and Papastefanou, 2006). Thus, in this study, the changes in deposition velocities and the residence times related only to the wet precipitation were considered. The deposition velocity (V_d) of fine aerosols can be determined by using the following equation (Dueñas et al.,

2005; McNeary and Baskaran, 2003; Papastefanou and Ioannidou, 1991).

$$V_d = \frac{\mathrm{F}}{C_s}$$

where F is the flux of ^{7}Be to the Earth's surface, and C_s is the activity of ^{7}Be in the surface air. The monthly deposition velocities using the ^{7}Be data from 1998 to 2017 were in the range from 0.22 cm·s^{-1} to 1.9 cm·s^{-1} with an average value of 0.63 cm·s^{-1} in this region. These deposition velocities for ^{7}Be are similar to those observed in southeastern Spain (0.07 cm·s^{-1} to 1.2 cm·s^{-1}, with a mean value of 0.4 cm·s^{-1}) (Dueñas et al., 2005). In general, the wet fallout accounts for most of the total depositional flux in areas with relatively high rainfall amount (Laguionie et al., 2014). Thus, the maximum deposition velocity value observed in July seems to be due to larger precipitation amounts in the summer monsoon season (Figure 3.12).

In order to examine the relative importance of depositional velocities in fine particle removal, the depositional velocities can be converted to the mean residence times of aerosols. The residence time can be defined as the time taken to remove all the PM10 in the atmosphere to the ground assuming no extra supply of PM10. If we assume that the mean depositional velocity (0.63 cm·s^{-1}) is equivalent to the global aerosol residence times (~8 days) based on ^{210}Bi/^{210}Pb ratios or aerosol modeling (Papastefanou, 2006), the residence times of fine aerosols estimated in this study could be in the order of winter (19 days), spring-fall (13 days), and summer (3 days). If the PM10 concentrations are proportional to the deposition velocities, the annual mean PM10 concentrations can be converted to the seasonal averages from 13 μg m^3 in summer to 68 μg m^3 in winter (spring: 47 μg m^3 and fall: 45 μg m^3). However, the maximum concentration of PM10 was observed in spring (58 μg m^3),

higher than that in winter (47 μg m^3). The higher PM10 concentrations in spring, relative to those expected from the aerosol residence times, seem to be due to more natural dust (Yellow dust) inputs in spring. The long-range transport of Yellow dust in spring is well known already in this region (Lee et al., 2006). The occurrence of PM10 in summer (34 μg m^3) is also 63% higher than expected from the short residence times of aerosols. Several previous studies have suggested that the increased PM10 concentrations could be observed due to the increased relative humidity (Al-Taai and Al-Ghabban, 2016; Hernandez et al., 2017). Thus, the higher PM10 measured than expected from the residence times in summer seems to be due to increased amounts of moisture in association with large precipitation events during the summer monsoon period. Our results suggest that if the input terms remain the same, the winter PM10 concentrations can be six-fold higher than the summer concentrations. Thus, ^{7}Be seems to provide important information on the fate of fine aerosols, excluding moisture effect, in the atmosphere.

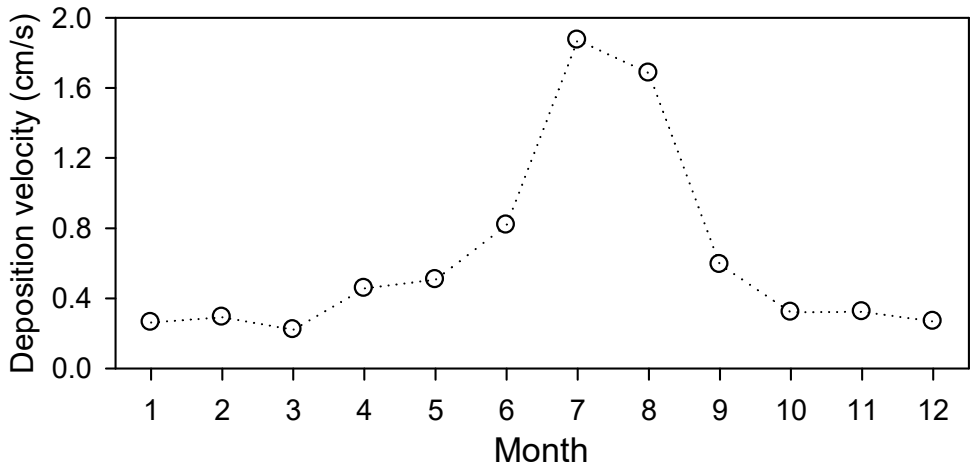

Figure 3.12. A monthly variation in estimated deposition velocities of fine aerosols using ^{7}Be. The monthly average deposition velocities are calculated using ^{7}Be activities in the surface air and wet deposition fluxes observed from 1998 to 2017.

3.4. Conclusions

^{7}Be activity data for the surface air and wet precipitation samples from 1998 to 2017 were analyzed. ^{7}Be activities in the surface air exhibited seasonal variations with increased values in spring due to the stratosphere-troposphere air exchange and decreased values in summer due to effective washouts by wet precipitation. The negative correlation between the ^{7}Be concentrations in the surface air and precipitation amount suggests that ^{7}Be activities are controlled mainly by precipitation. As such, the deposition velocity of ^{7}Be exhibited a minimum value in winter (0.27 $cm \cdot s^{-1}$) and the maximum value in summer (1.46 $cm \cdot s^{-1}$) due to the large amount of precipitation. This result implies that the PM10 concentrations in winter can be six-fold higher than those in summer if the input terms of PM10 remain the same over the year. More studies are necessary in order to determine the link between ^{7}Be and PM10 in the future.

4. Dispersion and removal characteristics of tritium originated from nuclear power plants in the atmosphere

4.1. Introduction

Tritium (^3H) is a radioactive isotope of hydrogen with a half-life of 12.32 years (Lucas and Unterweger, 2000) and is a low-energy pure-beta emitter with a maximum and average energy of 18.6keV and 5.7 keV, respectively. Tritium in the environment is naturally produced by cosmic-ray spallation mainly in the upper troposphere and lower stratosphere (Craig and Lal, 1961; Galeriu and Melintescu, 2010; Grosse et al., 1951; Masarik and Beer, 2009; Rozanski et al., 1991). In addition, the level of tritium was enhanced artificially by atmospheric tests of nuclear weapons in the late 1950s and early 1960s. Since the Extended Test Ban Treaty in 1963, the tritium levels in the atmosphere have decreased, approaching the natural tritium level nowadays (Guetat et al., 2011). However, there are additional sources of artificial tritium from the routine operations of nuclear power plants (NPPs). In general, the tritium production by heavy water reactors (HWRs) is tens of times higher than that by pressurized water reactors (PWRs). These nuclear facilities often become a significant source of tritium in the environment.

Tritium is released in the form of tritium gas (HT) and tritiated water (HTO) from a nuclear power plant (NPP), and most tritium in the environment exists in the HTO form. The HTO form of tritium is easily incorporated in the global hydrological

cycle. Therefore tritium has been used as a tracer in various fields including ocean circulation and ventilation (England and Maier-Reimer, 2001; Fine et al., 1981; Jenkins, 1996; Sarmiento, 1983), atmospheric and meteorological studies (Cauquoin et al., 2015; Moon et al., 1992; Rozanski et al., 1991; Yasunari and Yamazaki, 2009), and ground water movement (Santschi et al., 1987; Solomon et al., 1992; Von Buttlar and Wendt, 1958). Tritium that enters the hydrological cycle in the form of HTO can easily enter living organisms; it can enter the human body by ingestion and inhalation. In order to identify and counteract the radiological effect from tritium, many studies have been conducted around nuclear facilities (Fujita et al., 2007; Matsuura et al., 1995). In addition, several studies were performed on the food-chain transfer of tritium (Ciffroy et al., 2006), impact of NPPs on the river environment (Hanslík et al., 2009), verification of the washout model (Köllő et al., 2011; Kim et al., 2003; Piskunov et al., 2012; Tokuyama and Oonishi, 1997), transfer of tritium from water to tissue-free water tritium (TFWT) of organisms in the NPP cooling reservoir (Baeza et al., 2009), conversion of HTO in air to organically bound tritium (OBT) in plants in the vicinity of a nuclear facility (Vichot et al., 2008), and spatial and temporal distributions of tritium around nuclear facilities (Chae et al., 2011; Connan et al., 2017; Miljević et al., 2000).

Although various studies have been performed on the distributions of tritium in the atmosphere around nuclear facilities, the factors controlling the long-term spatio-temporal changes in tritium near nuclear facilities are poorly understood. Therefore, in this study, we evaluated (1) the dispersion characteristics and (2) removal proportions to the ground by precipitations for tritium released from the NPPs based on extensive monitoring data of tritium in water vapor and precipitation obtained in

the vicinity of the Wolsong NPP site. This information may provide important information on the modelling of tritium behavior and radiation protection around NPPs in normal operation as well as emergency situations.

4.2. Materials and Methods

4.2.1. Study area

The Wolsong NPP site is located on the southeastern coast of the Korean Peninsula. The site is surrounded by small mountains on the west side and borders on the East Sea (Japan Sea) on the east side. In the Wolsong NPP site, the Wolsong NPP Unit 1 began operation in April 1983, and the Wolsong NPP Units 2, 3 and 4, Shinwolsong NPP Units 1 and 2 have operated commercially since July 1997, July 1998, October 1999, July 2012, and July 2015 respectively. Among the six NPPs, the Wolsong NPP Units 1, 2, 3, and 4 are HWRs (CANDU-type reactors), while the Shinwolsong NPP Units 1 and 2 are PWRs. The annual tritium discharge amounts from the Wolsong NPP site ranged 125–403 TBq during 2001–2015. Although the amount of discharged tritium has been reduced by the operation of a tritium removal facility since 2007, a considerable amount of tritium over 100 TBq per year has still been released into the environment.

Several studies have been performed around the Wolsong NPP site. When only the Wolsong NPP Unit 1 was operating, the TFWT and OBT activity concentrations were found to be affected by the released amount of tritium (Kim et al., 2000a; Kim et al., 1998). The annual effective dose was estimated to be approximately 1.3 μSv/y in the vicinity of the site (within 1.6 km from the NPP) for environmental samples collected in 1992–1993 (Kim and Han, 1999). This dose level was significantly lower than the limit (1 $mSv \cdot y^{-1}$) of the effective dose to the general public recommended by the International Commission on Radiological Protection (ICRP) (ICRP, 2007). The distribution of tritium around this area has been reported (Chae et al., 2011; Kim et al., 1998).

4.2.2. Data acquisition

Basic data for tritium concentrations in water vapor and precipitation are available in the annual reports published by Korea Institute of Nuclear Safety (KINS) (KINS, 1998-2015). Atmospheric water-vapor tritium data are available for five sampling sites (N2, N4, N5, N7, and S2) from 1998 to 2015 (Figure 4.1). The results for the monthly sample collection periods at each site are shown in Tables 4.1 and 4.2. Precipitation tritium data are available for 17 sampling sites (N1–N10, S1–S7), located within 0.6–22 km from the Wolsong NPP site (Figure 4.1). Meteorological data are available from Korea Hydro &Nuclear Power (KHNP), which manages the meteorological station located in the Wolsong NPP site.

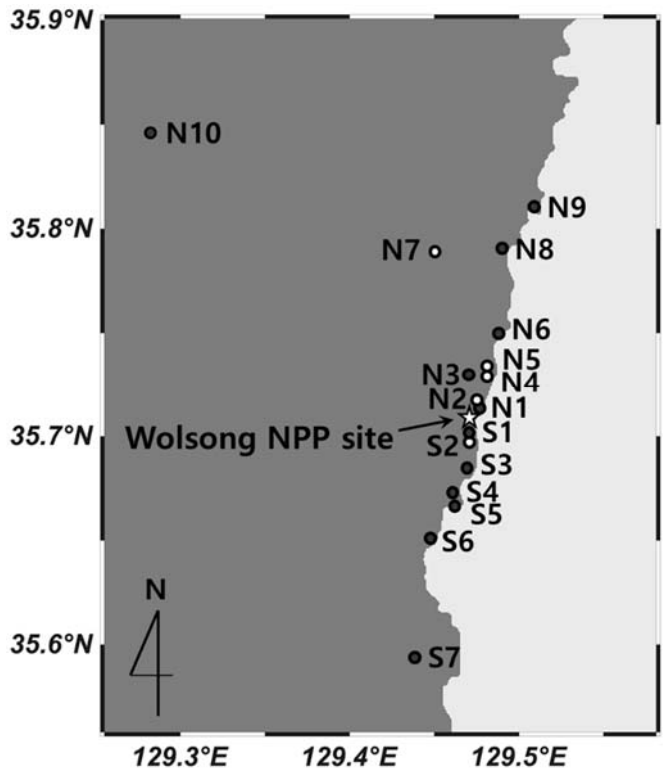

Figure 4.1. Map of the sampling stations around the Wolsong NPP site. The star, open circles, and closed circles represent the Wolsong NPP site and sampling stations for both water vapor and precipitation, and precipitation, respectively.

Table 4.1. Concentrations of tritium in the water vapor around the Wolsong NPP.

Station	Location		Range (Bq/L)	GM[a] (Bq/L)	SD[a] (Bq/L)	Period
	Cardinal direction	Distance (km)				
N2	N	0.9	68 - 2200	431	517	2003.4 - 2008.12
N4	NNE	1.8	37 - 1810	262	358	1998.1 - 2003.3
N5	NNE	2.2	14 - 798	120	142	1998.1 - 2015.12
N7	NNW	8.8	2.2 - 67	12	12	2008.5 - 2015.12
S2	SSW	1.7	18 - 645	75	77	1998.1 - 2015-12

[a] Geometric mean (GM), standard deviation (SD).

Table 4.2. Concentrations of tritium in the precipitation around the Wolsong NPP.

Station	Location		Range (Bq/L)	GM[a] (Bq/L)	SD[a] (Bq/L)	Period
	Cardinal direction	Distance (km)				
N1	NNE	0.6	0.8 - 834	99	207	2001.1-2015.12
N2	N	0.9	1.2 - 490	56	144	2003.4-2008.12
N3	N	1.7	2.0 - 113	16	27	2008.1-2015.12
N4	NNE	1.8	1.2 - 545	48	129	1998.1-2003.3
N5	NNE	2.2	0.3 - 804	28	90	1998.1-2011.12
N6	NNE	4.1	0.8 - 135	11	24	1998.1-2015.12
N7	NNW	8.8	1.3 - 23	4.7	5.2	2008.3-2015.12
N8	N	8.9	0.8 - 66	6.0	10	1998.1-2015.12
N9	NNE	11	0.8 - 51	4.8	8.1	1998.1-2011.12
N10	NW	22	0.8 - 10	2.3	1.7	1998.1-2011.12
S1	SSW	0.9	1.7 - 1090	149	200	1998.1-2011.12
S2	SSW	1.7	1.5 - 740	56	97	1998.1-2015.12
S3	S	2.4	1.8 - 604	44	80	1998.1-2011.12
S4	SSW	4.2	0.8 - 222	18	29	1998.1-2015.12
S5	S	4.9	1.5 - 147	19	25	1998.1-2011.12
S6	SSW	6.8	1.2 - 87	10	13	1998.1-2011.12
S7	SSW	14	0.8 - 62	5.7	6.1	1998.1-2015.12

4.2.3. Analytical Methods

We briefly describe the analytical method used for the monitoring. Atmospheric water samples were collected using an air sampler, which includes a series of molecular sieve adsorption columns (ÖStlund and Mason, 1974). The sampler was installed approximately 1 m above the ground with a flow rate of 0.52–1 L/min. Precipitation samples were collected using a rainwater sampler with a surface area of 0.1 m^2. The sampler was positioned at a height of 1 m above the ground. HTO was extracted from the molecular sieve column (45 cm × 5 cm i.d.) by heating at 450°C for 2 h in the laboratory. After distillation, 10 mL of the water sample was added to a 20-mL Perfluoroalkoxy (PFA) vial, together with 10 ml of Ultima gold LLT cocktail (Packard, USA); the mixture was then sufficiently mixed. The prepared sample was measured 10 times for 50 minutes by using a liquid scintillation counter (1220 Quantulus, PerkinElmer). The rainwater samples were distilled, and the method used for the tritium analysis in a water vapor sample was employed.

4.3. Results and Discussion

4.3.1. Tritium activity in water vapor

The distances from the sampling stations, N2, N4, N5, N7, and S2, to the Wolsong NPP site were in the range of 0.88 km to 8.79 km (Figure 4.1). The activity concentrations of tritium in water vapor collected monthly from 1998 to 2015 around the NPP site significantly varied (2.2 Bq/L to 2202 Bq/L, geometric mean (GM): 91 Bq/L, SD: 279 Bq/L, n = 649) at all sampling stations (Figure 4.2). This range is two orders of magnitude higher than the background tritium levels of 0.69 Bq/L and 1.86 Bq/L measured at Kumamoto and Fukuoka, Japan (Momoshima et al., 2007; Okai et al., 1999), respectively. However, it is comparable to the tritium activity concentration range of 16–2,468 Bq/L in water vapor reported by Miljević et al. (2000) around the Vinča Institute of Nuclear Sciences (VINS).

The mean concentrations of tritium in the water vapor at the four sampling stations located northward of the NPP rapidly decreased with distance from the NPP site. At the site located 1.7 km southward from the NPP (S2), the geometric mean concentration of tritium in the water vapor was 75 Bq/L (SD: 77 Bq/L), which was considerably lower than that (GM: 262 Bq/L; SD: 249 Bq/L) estimated at N4, located 1.8 km northward from the NPP site. The sampling station S2 is located on a mountainous terrain in the north and west, while the station N4 is on a relatively flat terrain without high mountains in the vicinity. The lower water-vapor tritium activities observed in the south seem to be associated with the difference in local topographies. Therefore, the tritium distributions in the atmosphere seem to be affected by various meteorological and topographical conditions.

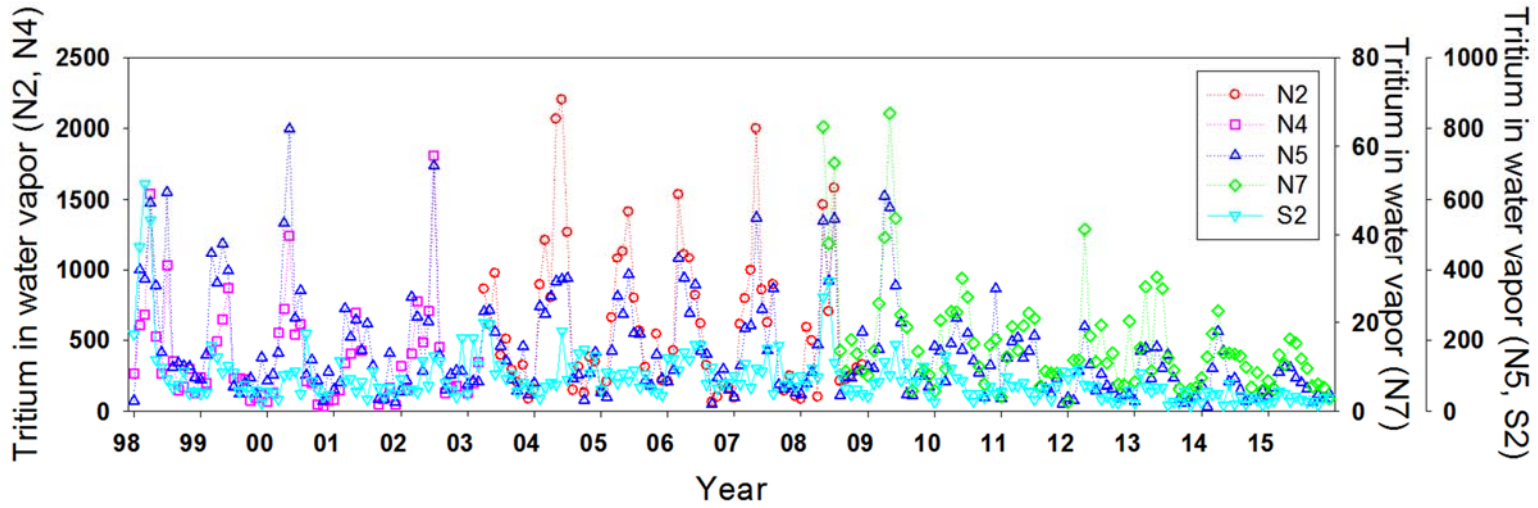

Figure 4.2. Time series of the tritium concentrations (Bq/L) in the water vapor at the sampling stations N2, N4, N7, and S2 during the sampling periods

4.3.2. Temporal variation of tritium activity in water vapor

The average concentrations of tritium in the water vapor for each month during the sampling period exhibited significant monthly variations, with considerably higher values in spring (Figure 4.3–4.5). Although the amount of tritium released from the NPPs could be the major factor affecting the activity, the monthly tritium concentrations in the water vapor did not exhibit significant correlations with the tritium emission amounts (N2: $r^2 = 0.04$, N4: $r^2 = 0.17$, N5: $r^2 = 0.04$, N7: $r^2 = 0.70$, S2: $r^2 = 0.01$). In addition, the monthly variation of the tritium concentration in the water vapor (relative standard deviation (RSD): 65% at N2) was approximately 7 times larger than the monthly variation released (monthly) from the Wolsong NPP site (RSD: 9% at N2). The variations of the tritium concentrations in the water vapor were larger (RSD: 65% (N2), 72% (N4), 58% (N5), and 51% (N7)) at the sampling stations located northward of the Wolsong NPP site than that at the station S2 (RSD: 28%) located southward of the NPP site. These observations reveal that the monthly variations of tritium in the water vapor appear to be insignificantly affected by the amount of tritium released from the NPP site.

However, the average tritium concentrations in the water vapor for each month during the sampling periods exhibited significant correlations with the frequency (%) of the wind directions (Figure 4.6–4.8). The highest correlation coefficient between the monthly frequency (%) of the southwest wind and tritium concentration was observed at the N5 station in 2005 ($r^2 = 0.86$). At the station S2, located southward of the NPP site, the maximum value of the correlation coefficients ($r^2 = 0.48$; wind direction: northeast (NE); sampling period: 2007) was significantly lower than that

at the northern stations (Figure 4.9). This seems to be associated with the local topographic differences between the stations located northward and southward from the NPP site. Our results suggest that the distributions of the tritium concentrations in the water vapor at locations near the NPP site are affected predominantly by wind directions, indicating that the effects of other factors, such as sea salts, soils, and organisms, are negligible.

Unlike the monthly tritium variation, the annual geometric means of the tritium concentrations in the water vapor were strongly correlated ($r^2 = 0.76$ at N5, $r^2 = 0.86$ at N7, and $r^2 = 0.81$ at S2) with the annual tritium emission amount from the NPPs (Figure 4.10). The slopes of the linear regression lines in the scatter plots between the annual averages of the tritium concentrations and amount of annual tritium emissions increase with the decrease of the distance from the NPP site (Figure 4.10). In contrast, the correlation coefficients between the annual average tritium concentrations and amount of tritium emissions were higher at the stations with lower tritium concentrations, indicating that the tritium activities in the water vapor are more dynamic at sampling stations closer to the NPP site.

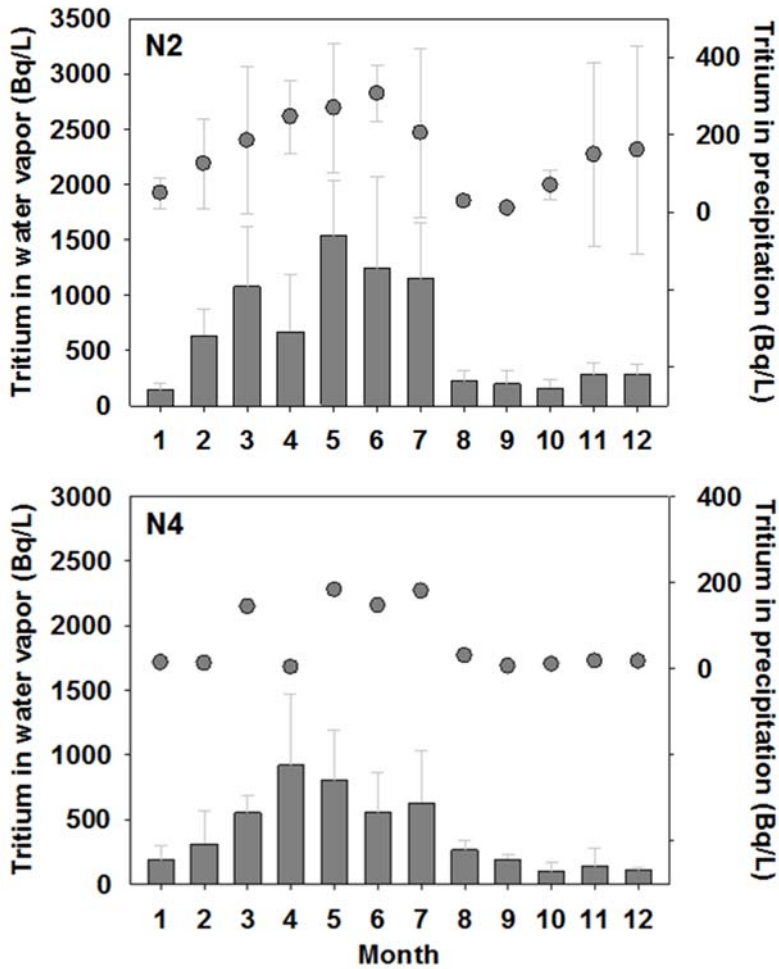

Figure 4.3. Average concentrations of tritium for each month in the water vapor during the sampling periods (2004, 2006, and 2008 at N2; 1998, 1999, and 2000 at N4) and precipitation during the sampling periods (2004, 2006, and 2008 at N2; 2001 at N4). The bars and circles represent water vapor and precipitation, respectively. The error bars represent the standard deviations.

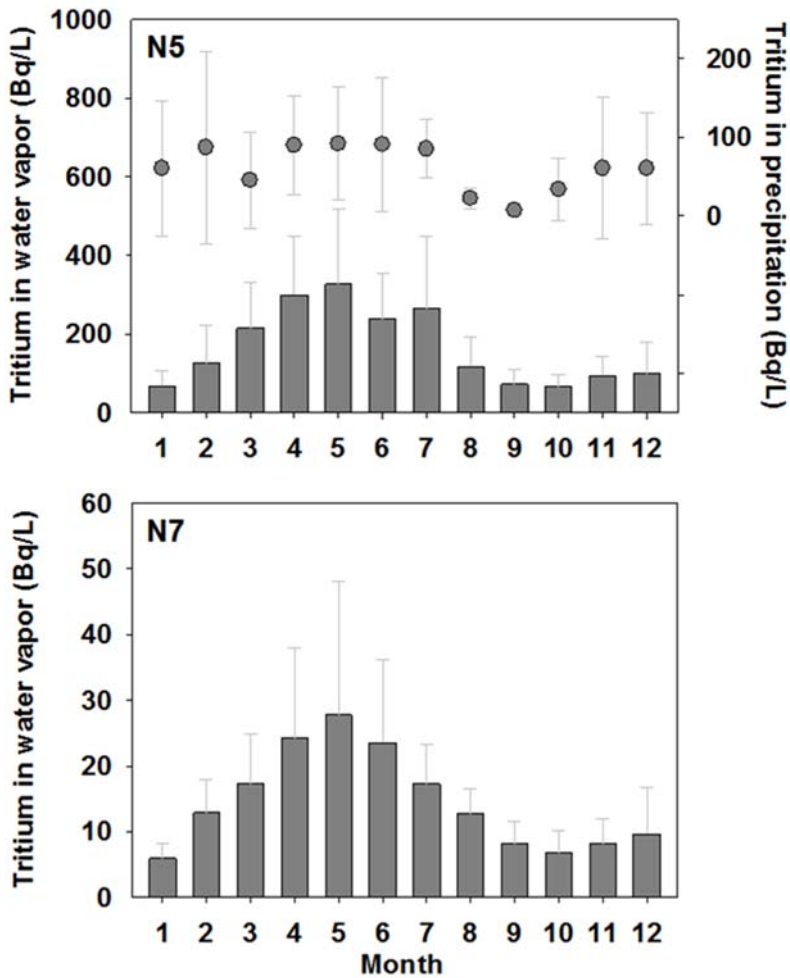

Figure 4.4. Average concentrations of tritium for each month in the water vapor during the sampling periods (1998–2015 at N5; 2009–2010 and 2012–2015 at N7) and precipitation during the sampling periods (2003–2004, 2006, 2008, and 2010 at N5). The bars and circles represent water vapor and precipitation, respectively. The error bars represent the standard deviations.

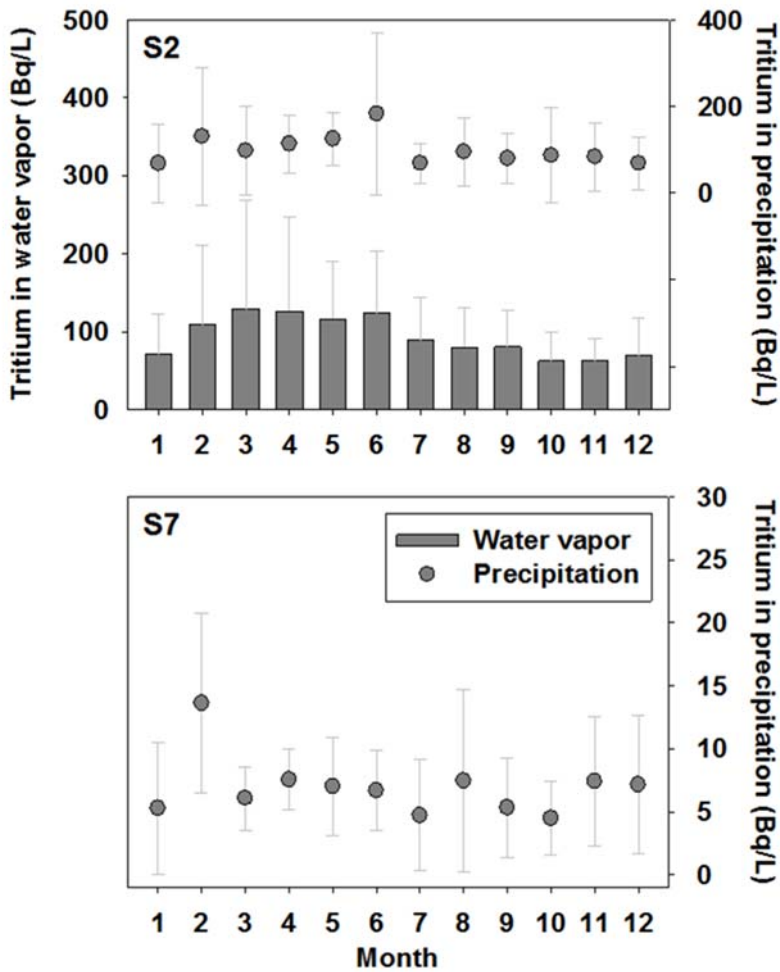

Figure 4.5. Average concentrations of tritium for each month in the water vapor during the sampling periods (1998–2000 and 2002–2015 at S2) and precipitation during the sampling periods (2001, 2003–2004, 2006, and 2008–2011 at S2; 2001, 2003, 2006, 2009, and 2015 at S7). The bars and circles represent water vapor and precipitation, respectively. The error bars represent the standard deviations.

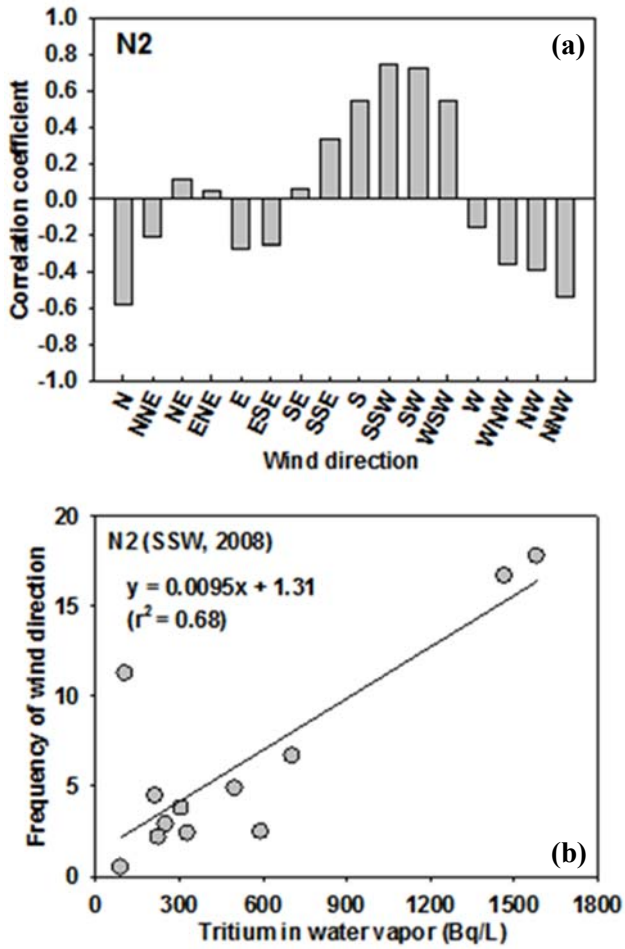

Figure 4.6. Average correlation coefficients between the concentrations of tritium in the water vapor and frequency of wind directions (%) (a) and plots of the monthly activity concentrations of tritium in the water vapor against the frequency of wind directions (%) for one year (N2:south-southwest (SSW) wind, in 2008) (b).

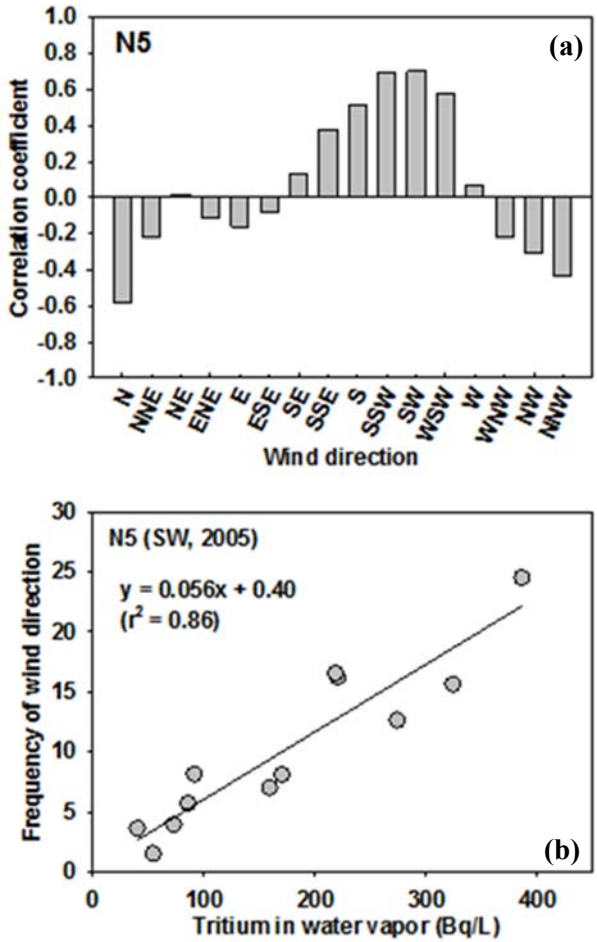

Figure 4.7. Average correlation coefficients between the concentrations of tritium in the water vapor and frequency of wind directions (%) (a) and plots of the monthly activity concentrations of tritium in the water vapor against the frequency of wind directions (%) for one year (N5: southwest (SW) wind, in 2005) (b).

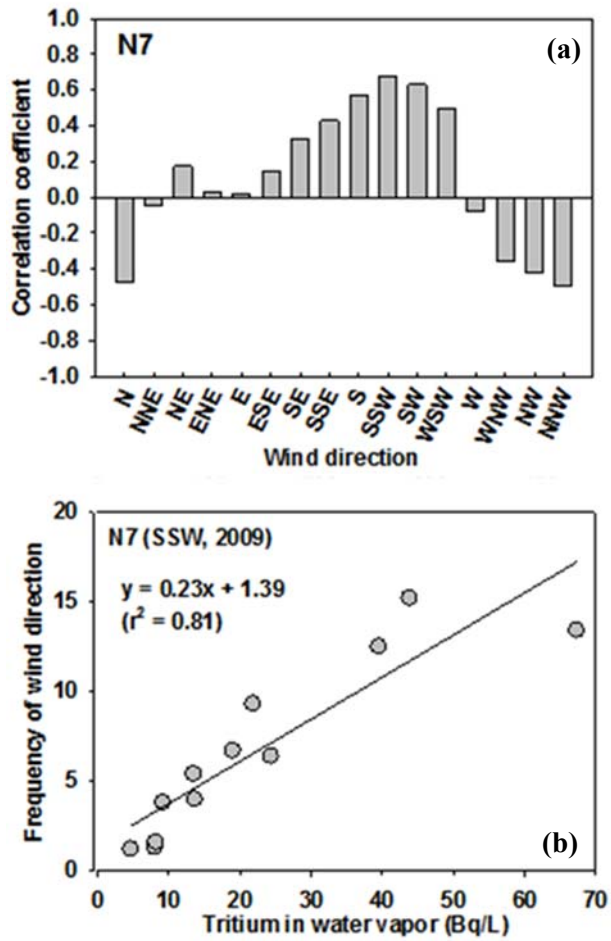

Figure 4.8. Average correlation coefficients between the concentrations of tritium in the water vapor and frequency of wind directions (%) (a) and plots of the monthly activity concentrations of tritium in the water vapor against the frequency of wind directions (%) for one year (N7: SSW wind, in 2009) (b).

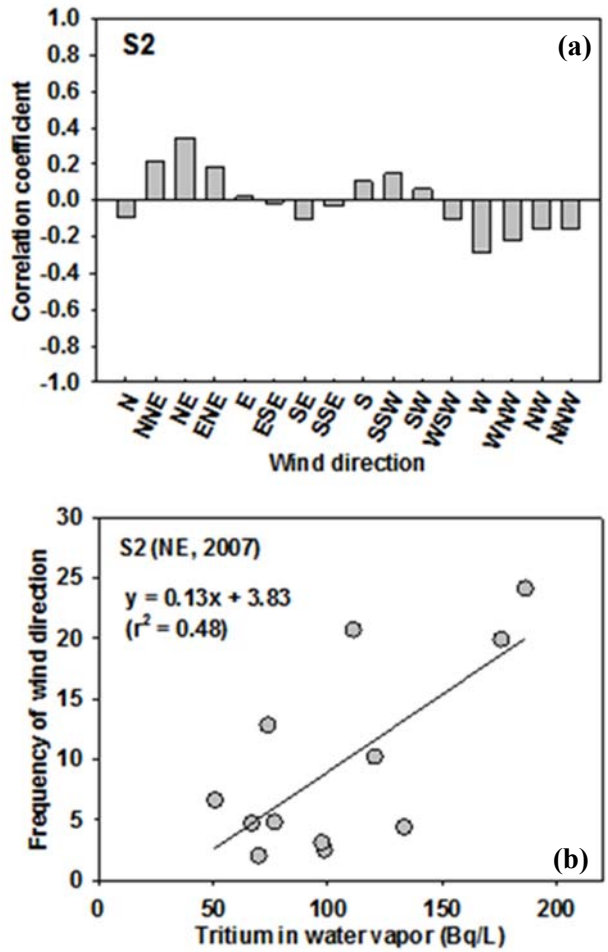

Figure 4.9. Average correlation coefficients between the concentrations of tritium in the water vapor and frequency of wind directions (%) (a) and plots of the monthly activity concentrations of tritium in the water vapor against the frequency of wind directions (%) for one year (S2: NE wind, in 2007) (b).

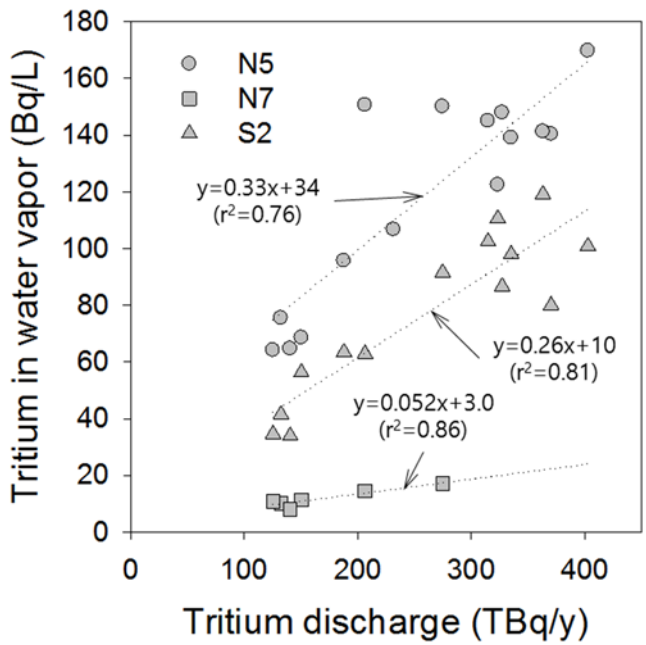

Figure 4.10. Plots of the annual geometric mean concentrations in the water vapor during the sampling periods (2001–2015 at N5; 2009–2010 and 2012–2015 at N7; 2002–2015 at S2) against the amounts of tritium released annually from the Wolsong NPP.

4.3.3. Tritium in the precipitation

The concentrations of tritium in the precipitation were in the range of 0.3–1090 Bq/L with a geometric mean of 19 Bq/L (SD: 116 Bq/L; n = 2,404) for all sampling stations (Table 4.2). These values are comparable with those in the precipitation (1.7–1554 Bq/L) observed around the Wolsong NPP site from 1993 to 1995 when only the Wolsong Unit 1 operated (Kim et al., 1998). However, these tritium levels are approximately two orders of magnitude higher than the background level (1.05 Bq/L) observed at 15 national monitoring stations in Korea (KINS, 2006). These levels are also significantly higher than those reported for rain water (0.8–8.9 Bq/L) around nuclear facilities in Japan (Matsuura et al., 1995), precipitation (0.6–5.9 Bq/L) around the nuclear power plant in Hungary (Köllő et al., 2011), and precipitation (2.2–35.4 Bq/L) in the vicinity of the VINS (Miljević et al., 2000).

The tritium concentrations in the precipitation samples did not exhibit a strong positive correlation with the tritium concentrations in the water vapor at most sampling stations (N2: r^2 = 0.35, n = 65; N4: r^2 = 0.45, n = 53; N5: r^2 = 0.24, n = 155; N7: r^2 = 0.0007, n = 52; S2: r^2 = 0.39, n = 203). Although the concentrations of tritium in the precipitation could be affected primarily by those in the water vapor, they can also be influenced by the vertical distribution of tritium in the water vapor and meteorological conditions such as the number of events and amount of precipitation. In addition, the tritium concentrations in the water vapor could be changed by a removal to the ground owing to precipitation.

The average concentrations of tritium in the precipitation for each month during

the sampling period exhibited variations with higher values in spring and summer, similar with the seasonal variation in average concentration of tritium for each month in the water vapor (Figure 4.3–4.5). As mentioned above, although the tritium concentrations in the precipitation samples collected monthly did not exhibit a strong correlation with the tritium concentrations in the water vapor, the average concentrations of tritium for each month in the precipitation strongly correlated with the average concentrations of tritium for each month in the water vapor ($r^2 = 0.70$, $n = 12$ at N2; $r^2 = 0.61$, $n = 12$ at N5; $r^2 = 0.70$, $n = 12$ at S2). This result suggests that the overall monthly variation of tritium in the precipitation reflects the seasonal variation of tritium in the water vapor.

The annual geometric mean activity concentrations of tritium in the precipitation exhibited significant positive correlations (S1: $r^2 = 0.56$; S4: $r^2 = 0.88$; S7: $r^2 = 0.70$) with the amount of tritium annually released from the Wolsong NPP (Figure 4.11). The annual average tritium concentrations in the precipitations collected in 2006 tended to rapidly decrease with the increase of the distance from the Wolsong NPP site to the sampling sites (Figure 4.12). The annual mean activity concentration at the sampling station N10, 22 km away from the Wolsong NPP site, decreased to 2.59 Bq/L, which approaches the background level of 1.05 Bq/L (KINS, 2006).

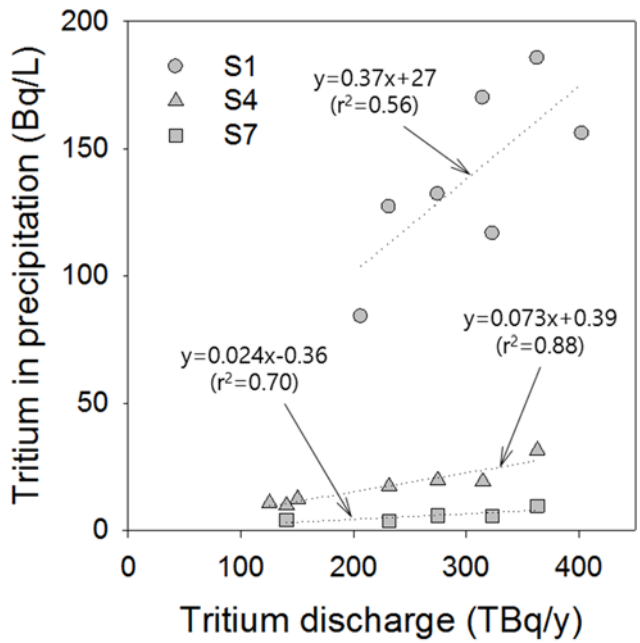

Figure 4.11. Plots of the annual geometric mean concentrations in the precipitation during the sampling periods (2001, 2003–2004, 2006 and 2008–2010 at S1; 2001, 2006, 2008–2009, 2012 and 2014–2015 at S4; 2001, 2003, 2006, 2009 and 2015 at S7) against the amounts of tritium released annually from the Wolsong NPP.

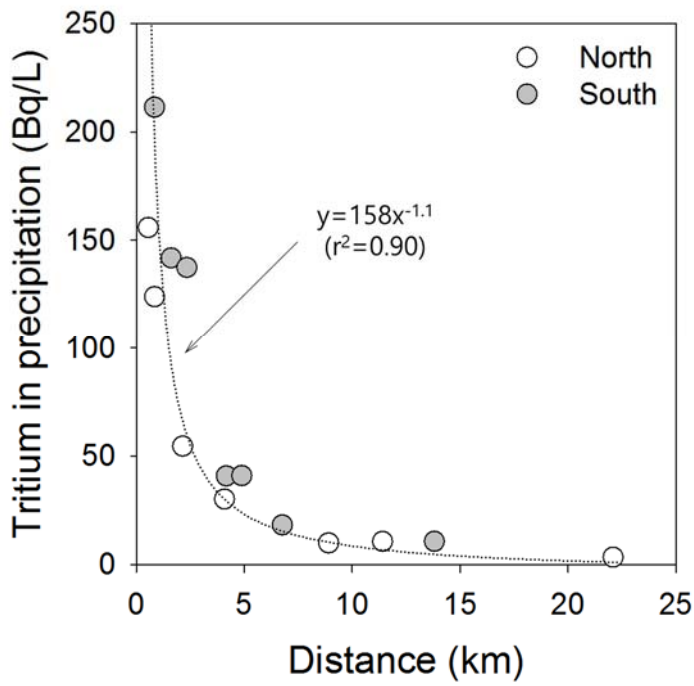

Figure 4.12. Plots of the annual average activity concentrations in 2006 against the distances from the Wolsong NPP site to the sampling stations. The open and closed circles represent the sampling stations northward and southward of the Wolsong NPP site, respectively.

4.3.4. Removal amounts of NPP tritium by wet precipitation to the ground

The removal amount of NPP tritium by wet precipitation to the ground can be calculated by estimating the total precipitation amount and the average tritium concentrations in precipitation for the given area (Eq. 1).

$$D = \sum_{r=1}^{n} \{\pi \cdot r^2 - \pi \cdot (r-1)^2\} \cdot A \cdot P \cdot 1000 \qquad (Eq.1)$$

where D is the removed amount (Bq) of tritium from water vapor in the air to the ground by wet precipitation in a circular area with a radius of n (m), r is the radius of a circular area around the Wolsong NPP site (m), A is the concentration of tritium in the precipitation at a distance of n from the Wolsong NPP site calculated using the regression line between the measured concentrations of tritium in the precipitation and distance from the Wolsong NPP site to the sampling station (Bq/L), and P is the amount of precipitation (m).

The removed amount of tritium by wet precipitation was estimated only for 2006 during which tritium data are available for almost all precipitation events. The number of data of concentrations of tritium in precipitation as a function of the distance was the highest in 2006 during the survey period. The amount of tritium deposition by wet precipitation for each month was calculated using Eq. (1). The background level of tritium in the precipitation (1.05 Bq/L) observed at 15 national monitoring stations in Korea (KINS, 2006) was subtracted from the concentrations

of tritium in the precipitation in Eq. (1).

The amounts of tritium deposition by wet precipitation for each month within a radius of 30 km around the Wolsong NPP site were in the range of 0.18 TBq (in December) to 7.8 TBq (in July) with relatively large monthly variations (RSD: 107%). As the monthly amount of tritium released from the Wolsong NPP site did not exhibit a large variation (RSD of 24%), the removed amount of tritium by precipitation for each month was not significantly affected by the amount of tritium emission. The largest and smallest values of the amount of tritium removed monthly by wet precipitation normalized to the amount of tritium released monthly from the Wolsong NPP site, were observed in July (31%) and March (0.5%), respectively. The amount of tritium removed by precipitation in summer (June, July, and August) was approximately 58% (16 TBq) of the annual removed amount of tritium. Approximately 28 TBq of tritium was removed to the ground by wet precipitation within an area with a radius of 30 km around the Wolsong NPP site for one year, which was approximately 8% of the annual amount of tritium (363 TBq) released from the Wolsong NPP site (Table 4.3). The proportions of the tritium amount monthly deposited by precipitation to the ground to the amount of tritium released monthly from the Wolsong NPP site exhibited a strong positive correlation ($r^2 = 0.69$) with the monthly precipitation amount. The proportions of the tritium amount monthly deposited by precipitation to the ground to the amount of tritium released monthly from the Wolsong NPP site increased by approximately 5% for every 100-mm increase of the monthly precipitation amount. This suggests that the tritium removal by precipitation is mainly controlled by the precipitation amount.

Table 4.3. Percentage ratio between the removed amount of tritium by wet precipitation and amount of tritium released from the Wolsong NPPs in 2006.

Month	The radius of the circular area around Wolsong NPP site		
	10 km	20 km	30 km
1	0.8	1.4	1.9
2	0.6	1.2	1.7
3	0.3	0.4	0.5
4	4.5	7.3	9.6
5	6.2	9.7	12
6	11	19	25
7	14	24	31
8	2.4	5.2	8.0
9	2.5	7.0	12
10	0.8	1.3	1.7
11	0.4	0.9	1.3
12	0.2	0.4	0.7
1 year	3.2	5.7	7.8

4.4. Conclusions

The dispersion and removal characteristics of tritium were investigated around the NPPs, which continuously discharge a considerable amount of tritium. The concentrations of tritium in water vapor and precipitation exhibited seasonal variations with increased values in spring and summer. The significant correlation between the concentrations of tritium in the water vapor and directional frequency of the wind revealed that the distribution of tritium in the water vapor was closely related with the wind direction. Although the concentrations of tritium observed monthly were not significantly correlated with the amount of tritium released monthly from NPPs, the annual geometric mean concentrations of tritium in the water vapor and precipitation appeared to vary with the amount of tritium released annually from NPPs. The annual removed amount of tritium to the ground by wet precipitation was approximately 8% of the amount of tritium released from the NPPs annually within an area with a radius of 30 km around the NPP site. Approximately 60% of the annual removed amount of tritium by wet precipitation was observed in the rainy season indicating that the main factor that controls the removal of tritium is the amount of precipitation. Further extensive studies are necessary in order to quantify the tritium distributions in various environmental states such as water vapor, ground water, soil, and plants around the NPP sites.

Bibliography

Al-Azmi, D., Sayed, A.M., Yatim, H.A., 2001. Variations in ^{7}Be concentrations in the atmosphere of Kuwait during the period 1994 to 1998. Applied Radiation and Isotopes 55, 413-417.

Al-Taai, O.T., Al-Ghabban, Z.M., 2016. The influence of relative humidity on concentrations (PM10, TSP) in Baghdad city. Modern Environmental Science and Engineering 2, 111-122.

Anh, H.L., Anh, V.T., Giap, T.V., Hong Thinh, N.T., Minh, T.K., Hoai, V., 2018. Monitoring of tritium concentration in Hanoi's precipitation from 2011 to 2016. Journal of Environmental Radioactivity 192, 143-149.

Araguas, L.A., Danesi, P., Froehlich, K., Rozanski, K., 1996. Global monitoring of the isotopic composition of precipitation. Journal of Radioanalytical and Nuclear Chemistry 205, 189-200.

Azahra, M., Camacho-García, A., González-Gómez, C., López-Peñalver, J.J., El Bardouni, T., 2003. Seasonal ^{7}Be concentrations in near-surface air of Granada (Spain) in the period 1993–2001. Applied Radiation and Isotopes 59, 159-164.

Baeza, A., García, E., Paniagua, J.M., Rodríguez, A., 2009. Study of the comparative dynamics of the incorporation of tissue free-water tritium (TFWT) in bulrushes (Typha latifolia) and carp (Cyprinus carpio) in the Almaraz nuclear power plant cooling reservoir. Journal of Environmental Radioactivity 100, 209-214.

Baskaran, M., Coleman, C.H., Santschi, P.H., 1993. Atmospheric depositional fluxes

of ^{7}Be and ^{210}Pb at Galveston and College Station, Texas. Journal of Geophysical Research: Atmospheres 98, 20555-20571.

Begemann, F., Libby, W.F., 1957. Continental water balance, ground water inventory and storage times, surface ocean mixing rates and world-wide water circulation patterns from cosmic-ray and bomb tritium. Geochimica et Cosmochimica Acta 12, 277-296.

Benitez-Nelson, C.R., Buesseler, K.O., 1999. Phosphorus 32, phosphorus 37, beryllium 7, and lead 210: Atmospheric fluxes and utility in tracing stratosphere/troposphere exchange. Journal of Geophysical Research: Atmospheres 104, 11745-11754.

Bolin, B., 1958. On the use of tritium as a tracer for water in nature. In: Proceedings of the Second United Nations Conference on the Peaceful Uses of Atomic Energy, Geneva, Switzerland. 336-343.

Brost, R.A., Feichter, J., Heimann, M., 1991. Three-dimensional simulation of ^{7}Be in a global climate model. Journal of Geophysical Research: Atmospheres 96, 22423-22445.

Cannizzaro, F., Greco, G., Raneli, M., Spitale, M.C., Tomarchio, E., 2004. Concentration measurements of ^{7}Be at ground level air at Palermo, Italy—comparison with solar activity over a period of 21 years. Journal of Environmental Radioactivity 72, 259-271.

Cauquoin, A., Jean-Baptiste, P., Risi, C., Fourré, É., Stenni, B., Landais, A., 2015. The global distribution of natural tritium in precipitation simulated with an Atmospheric General Circulation Model and comparison with observations. Earth and Planetary Science Letters 427, 160-170.

Chae, J.-S., Lee, S.-K., Kim, Y., Lee, J.-M., Cho, H.-J., Cho, Y.-W., Yun, J.-Y., 2011.

Distribution of tritium in water vapour and precipitation around Wolsung nuclear power plant. Radiation Protection Dosimetry 146, 330-333.

Chatani, S., Morikawa, T., Nakatsuka, S., Matsunaga, S., Minoura, H., 2011. Development of a framework for a high-resolution, three-dimensional regional air quality simulation and its application to predicting future air quality over Japan. Atmospheric Environment 45, 1383-1393.

Cho, H.-M., Hong, Y.-L., Kim, G., 2011. Atmospheric depositional fluxes of cosmogenic ^{35}S and ^{7}Be: Implications for the turnover rate of sulfur through the biosphere. Atmospheric Environment 45, 4230-4234.

Ciffroy, P., Siclet, F., Damois, C., Luck, M., 2006. A dynamic model for assessing radiological consequences of tritium routinely released in rivers. Application to the Loire River. Journal of Environmental Radioactivity 90, 110-139.

Clark, I.D., Fritz, P., 1997. Environmental Isotopes in Hydrogeology. Lewis, New York.

CNSC, 2009. Investigation of the Environmental Fate of Tritium in the Atmosphere-Part of the Tritium Studies Project, INFO-0792. Canadian Nuclear Safety Commission, Ottawa, Canada.

Connan, O., Hébert, D., Solier, L., Maro, D., Pellerin, G., Voiseux, C., Lamotte, M., Laguionie, P., 2017. Atmospheric tritium concentrations under influence of AREVA NC La Hague reprocessing plant (France) and background levels. Journal of Environmental Radioactivity 177, 184-193.

Craig, H., Gordon, L.I., 1965. Deuterium and oxygen 18 variations in the ocean and the marine atmosphere. In: Tongiorigi, E. (Ed.), Stable isotopes in oceanographic studies and paleotemperatures. Lab di Geologia Nucleare, Pisa. 9-130.

Craig, H., Lal, D., 1961. The Production Rate of Natural Tritium. Tellus 13, 85-105.

Dueñas, C., Fernández, M.C., Carretero, J., Liger, E., Cañete, S., 2005. Deposition velocities and washout ratios on a coastal site (southeastern Spain) calculated from 7Be and 210Pb measurements. Atmospheric Environment 39, 6897-6908.

Duliu, O.G., Varlam, C., Shnawaw, M.D., 2018. 18 years of continuous observation of tritium and atmospheric precipitations in Ramnicu Valcea (Romania): A time series analysis. Journal of Environmental Radioactivity 190-191, 105-110.

Ehhalt, D.H., Rohrer, F., Schauffler, S., Pollock, W., 2002. Tritiated water vapor in the stratosphere: Vertical profiles and residence time. Journal of Geophysical Research: Atmospheres 107, ACH 8-1-ACH 8-15.

England, M.H., Maier-Reimer, E., 2001. Using chemical tracers to assess ocean models. Reviews of Geophysics 39, 29-70.

Feely, H.W., Larsen, R.J., Sanderson, C.G., 1989. Factors that cause seasonal variations in Beryllium-7 concentrations in surface air. Journal of Environmental Radioactivity 9, 223-249.

Fine, R.A., Reid, J.L., Östlund, H.G., 1981. Circulation of Tritium in the Pacific Ocean. Journal of Physical Oceanography 11, 3-14.

Fujita, H., Kokubun, Y., Koarashi, J., 2007. Environmental Tritium in the Vicinity of Tokai Reprocessing Plant. Journal of Nuclear Science and Technology 44, 1474-1480.

Galeriu, D., Melintescu, A., 2010. Radionuclides in the environment. John Wiley & Sons Ltd., West Sussex, England.

Gat, J., Mook, W., Meijer, H., 2001. Tritium in the Atmosphere, in: Gat, J.R., Mook,

W.G., Meijer, H.A.J. (Eds.), Environmental Isotopes in the Hydrological Cycle, Principles and Applications Vol. II, IAEA, Vienna.

Gröning, M., Rozanski, K., 2003. Uncertainty assessment of environmental tritium measurements in water. Accreditation and Quality Assurance 8, 359-366.

Graustein, W.C., Turekian, K.K., 1996. ^{7}Be and ^{210}Pb Indicate an upper troposphere source for elevated ozone in the summertime subtropical free troposphere of the eastern North Atlantic. Geophysical Research Letters 23, 539-542.

Grosse, A.V., Johnston, W.M., Wolfgang, R.L., Libby, W.F., 1951. Tritium in Nature. Science 113, 1-2.

Guetat, P., Boyer, C., Tognelli, A., Duda, J.M., 2011. 50 Years Environmental Tritium Transfer Review in the Vicinity of French Research Centre. Fusion Science and Technology 60, 1238-1243.

Hanslík, E., Ivanovová, D., Jedináková-Křížová, V., Juranová, E., Šimonek, P., 2009. Concentration of radionuclides in hydrosphere affected by Temelín Nuclear Power Plant in Czech Republic. Journal of Environmental Radioactivity 100, 558-563.

Harms, P.A., Visser, A., Moran, J.E., Esser, B.K., 2016. Distribution of tritium in precipitation and surface water in California. Journal of Hydrology 534, 63-72.

Hayashi, Y., Momoshima, N., Maeda, Y., Kakiuchi, H., 1999. Relation between tritium concentration and chemical composition in rain at Fukuoka. Journal of Radioanalytical and Nuclear Chemistry 239, 517-522.

Herczeg, A.l., Imboden, D.M., 1988. Tritium hydrologic studies in four closed-basin lakes in the Great Basin, USA. Limnology and Oceanography 33, 157-173.

Hernandez, G., Berry, T.-A., Wallis, S.L., Poyer, D., 2017. Temperature and humidity

effects on particulate matter concentrations in a sub-tropical climate during winter. International Proceedings of Chemical, Biological and Environmental Engineering 102.

Huneeus, N., Chevallier, F., Boucher, O., 2012. Estimating aerosol emissions by assimilating observed aerosol optical depth in a global aerosol model. Atmos. Chem. Phys. 12, 4585-4606.

IAEA, 1992. Statistical treatment of data on environmental isotopes in precipitation. Technical Report Series 331, IAEA Vienna, 781 pp.

IAEA, 2018. Global Network of Isotopes in Precipitation. Water Resources Programme. <http://www-naweb.iaea.org/napc/ih/IHS_resources_gnip.html>.

IAEA/WMO, 2018. Global Network of Isotopes in Precipitation. The GNIP Database. <http://www.iaea.org/water>.

ICRP, 2007. The 2007 Recommendations of the International Commission on Radiological Protection, ICRP Publication 103.

Igarashi, Y., Hirose, K., Otsuji-Hatori, M., 1998. Beryllium-7 Deposition and Its Relation to Sulfate Deposition. Journal of Atmospheric Chemistry 29, 217-231.

In, H.-J., Kim, Y.P., 2010. Estimation of the aerosol optical thickness distribution in the Northeast Asian forest fire episode in May 2003: Possible missing emissions. Atmospheric Research 98, 261-273.

Ioannidou, A., 2011. Activity size distribution of ^{7}Be in association with trace metals in the urban area of the city of Thessaloniki, Greece. Atmospheric Environment 45, 1286-1290.

Ioannidou, A., Papastefanou, C., 2006. Precipitation scavenging of ^{7}Be and ^{137}Cs

radionuclides in air. Journal of Environmental Radioactivity 85, 121-136.

Jenkins, W.J.S., W. M. , 1996. Transient tracers track ocean climate signals. Oceanus 39, 29-32.

Jerrett, M., Arain, A., Kanaroglou, P., Beckerman, B., Potoglou, D., Sahsuvaroglu, T., Morrison, J., Giovis, C., 2004. A review and evaluation of intraurban air pollution exposure models. Journal Of Exposure Analysis And Environmental Epidemiology 15, 185.

Köllő, Z., Palcsu, L., Major, Z., Papp, L., Molnár, M., Ranga, T., Dombóvári, P., Manga, L., 2011. Experimental investigation and modelling of tritium washout by precipitation in the area of the nuclear power plant of Paks, Hungary. Journal of Environmental Radioactivity 102, 53-59.

Kathren, R.L., 1984. Radioactivity in the Environment: Sources, distribution, and surveillance. Harwood Academic Publishers, Chur, Switzerland.

Kim, C.-K., Han, M.-J., 1999. Dose assessment and behavior of tritium in environmental samples around Wolsong nuclear power plant. Applied Radiation and Isotopes 50, 783-791.

Kim, C.-K., Lee, S.-K., Rho, B.-H., Lee, Y.G., 2000a. Environmental distribution and behavior of ^{3}H and ^{14}C around Wolsong nuclear power plants. Health Physics 78, 693-699.

Kim, C.-K., Rho, B.-H., Lee, K.J., 1998. Environmental tritium in the areas adjacent to Wolsong nuclear power plant. Journal of Environmental Radioactivity 41, 217-231.

Kim, C.K., Lee, S.K., Rho, B.H., Park, G.J., Kim, W., Kang, H.D., 2003. Washout of Tritiated Water Vapor by Precipitation in the Vicinity of Wolsong Nuclear Power Plant Site. J Radiat Prot 28, 337-330.

Kim, G., Alleman, L.Y., Church, T.M., 1999. Atmospheric depositional fluxes of trace elements, ^{210}Pb, and ^{7}Be to the Sargasso Sea. Global Biogeochemical Cycles 13, 1183-1192.

Kim, G., Hussain, N., Scudlark, J.R., Church, T.M., 2000b. Factors Influencing the Atmospheric Depositional Fluxes of Stable Pb, ^{210}Pb, and ^{7}Be into Chesapeake Bay. Journal of Atmospheric Chemistry 36, 65-79.

KINS, 1998-2015. The Annual Report on the Environmental Radiological Surveillance and Assessment around the Nuclear Facilities. Korea Institute of Nuclear Safety.

KINS, 1998-2017. Environmental Radioactivity Survey Data in Korea. Korea Institute of Nuclear Safety, KINS/ER-028, V. 20-39.

KINS, 2006. Environmental Radioactivity Suvey Data in Korea. Korea Institute of Nuclear Safety.

KMA, 2012. The climate atlas of Korea. Korea Meteorological Administration.

KMA, 2018. Meteorological data. Korea Meteorological Administration. <https://data.kma.go.kr/cmmn/main.do>.

Koch, D.M., Jacob, D.J., Graustein, W.C., 1996. Vertical transport of tropospheric aerosols as indicated by ^{7}Be and ^{210}Pb in a chemical tracer model. Journal of Geophysical Research: Atmospheres 101, 18651-18666.

Koo, Y.-S., Kim, S.-T., Yun, H.-Y., Han, J.-S., Lee, J.-Y., Kim, K.-H., Jeon, E.-C., 2008. The simulation of aerosol transport over East Asia region. Atmospheric Research 90, 264-271.

Laguionie, P., Roupsard, P., Maro, D., Solier, L., Rozet, M., Hébert, D., Connan, O., 2014. Simultaneous quantification of the contributions of dry, washout and rainout deposition to the total deposition of particle-bound ^{7}Be and ^{210}Pb on

an urban catchment area on a monthly scale. Journal of Aerosol Science 77, 67-84.

Lee, B.-K., Lee, H.K., Jun, N.-Y., 2006. Analysis of regional and temporal characteristics of PM10 during an Asian dust episode in Korea. Chemosphere 63, 1106-1115.

Lee, H.N., Wan, G., Zheng, X., Sanderson, C.G., Josse, B., Wang, S., Yang, W., Tang, J., Wang, C., 2004. Measurements of ^{210}Pb and ^{7}Be in China and their analysis accompanied with global model calculations of ^{210}Pb. Journal of Geophysical Research: Atmospheres 109.

Lee, S., Ho, C.-H., Choi, Y.-S., 2011. High-PM10 concentration episodes in Seoul, Korea: Background sources and related meteorological conditions. Atmospheric Environment 45, 7240-7247.

Li, N., Sioutas, C., Cho, A., Schmitz, D., Misra, C., Sempf, J., Wang, M., Oberley, T., Froines, J., Nel, A., 2003. Ultrafine particulate pollutants induce oxidative stress and mitochondrial damage. Environmental health perspectives 111, 455-460.

Lohmann, U., Feichter, J., 2005. Global indirect aerosol effects: a review. Atmos. Chem. Phys. 5, 715-737.

Lucas, L.L., Unterweger, M.P., 2000. Comprehensive Review and Critical Evaluation of the Half-Life of Tritium. Journal of Research of the National Institute of Standards and Technology 105, 541-549.

Martell, E.A., 1963. On the inventory of artificial tritium and its occurrence in atmospheric methane. Journal of Geophysical Research 68, 3759-3770.

Masarik, J., Beer, J., 1999. Simulation of particle fluxes and cosmogenic nuclide production in the Earth's atmosphere. Journal of Geophysical Research:

Atmospheres 104, 12099-12111.

Masarik, J., Beer, J., 2009. An updated simulation of particle fluxes and cosmogenic nuclide production in the Earth's atmosphere. Journal of Geophysical Research: Atmospheres 114..

Matsuoka, N., Hirai, E., Tagomori, H., Momoshima, N., Takashima, Y., 1994. Meteorological analysis of tritium concentrations in rain water collected in Fukuoka, Japan, from 1987–1991. Science of The Total Environment 145, 197-205.

Matsuura, K., Sasa, Y., Nakamura, C., Katagiri, H., 1995. Levels of tritium concentration in the environmental samples around JAERI TOKAI. Journal of Radioanalytical and Nuclear Chemistry 197, 295-307.

McNeary, D., Baskaran, M., 2003. Depositional characteristics of ^{7}Be and ^{210}Pb in southeastern Michigan. Journal of Geophysical Research: Atmospheres 108.

Megumi, K., Matsunami, T., Ito, N., Kiyoda, S., Mizohata, A., Asano, T., 2000. Factors, especially sunspot number, causing variations in surface air concentrations and depositions of ^{7}Be in Osaka, Japan. Geophysical Research Letters 27, 361-364.

Michel, R.L., 1976. Tritium inventories of the world oceans and their implications. Nature 263, 103.

Miljević, N., Šipka, V., Žujić, A., Golobočanin, D., 2000. Tritium around the Vinča Institute of Nuclear Sciences. Journal of Environmental Radioactivity 48, 303-315.

Miskel, J.A., 1971. PRODUCTION OF TRITIUM BY NUCLEAR WEAPONS. ; California Univ., Livermore. Lawrence Radiation Lab.

Momoshima, N., Yamaguchi, T., Toyoshima, T., Nagao, Y., Takahashi, M., Takamura,

M., Nakamura, Y., 2007. Tritium in the Atmospheric Environment. Journal of Nuclear and Radiochemical Sciences 8, 117-120.

Moon, S.-E., Kim, Y.-K., Park, J.-K., 1992. On the atmospheric conditions affecting the variation of tritium concentration in rainfall. Atmospheric Environment. Part A. General Topics 26, 2751-2758.

Morishima, H., Kawai, H., Koga, T., Niwa, T., 1985. The Trends of Global Tritium Precipitations. Journal of Radiation Research 26, 283-312.

NIER, 1999-2014. Annual report of air quality in Korea. National Institute of Environmental Research.

Okai, T., Momoshima, N., Takashima, Y., 1999. Variation of atmospheric tritium concentrations in three different chemical forms in Fukuoka, Japan. Journal of Radioanalytical and Nuclear Chemistry 239, 527-531.

ÖStlund, H.G., Mason, A.S., 1974. Atmospheric HT and HTO : I. Experimental procedures and tropospheric data 1968-72. Tellus 26, 91-102.

Ostro, B., Tobias, A., Karanasiou, A., Samoli, E., Querol, X., Rodopoulou, S., Basagaña, X., Eleftheriadis, K., Diapouli, E., Vratolis, S., Jacquemin, B., Katsouyanni, K., Sunyer, J., Forastiere, F., Stafoggia, M., 2015. The risks of acute exposure to black carbon in Southern Europe: results from the MED-PARTICLES project. Occupational and Environmental Medicine 72, 123-129.

Pan, J., Yang, Y.-L., Zhang, G., Shi, J.-L., Zhu, X.-H., Li, Y., Yu, H.-Q., 2011. Simultaneous observation of seasonal variations of beryllium-7 and typical POPs in near-surface atmospheric aerosols in Guangzhou, China. Atmospheric Environment 45, 3371-3380.

Papastefanou, C., 2006. Residence time of tropospheric aerosols in association with

radioactive nuclides. Applied Radiation and Isotopes 64, 93-100.

Papastefanou, C., Ioannidou, A., 1991. Depositional fluxes and other physical characteristics of atmospheric beryllium-7 in the temperate zones (40°N) with a dry (precipitation-free) climate. Atmospheric Environment. Part A. General Topics 25, 2335-2343.

Papastefanou, C., Ioannidou, A., 1995. Aerodynamic size association of ^{7}Be in ambient aerosols. Journal of Environmental Radioactivity 26, 273-282.

Parekh, P.P., Khwaja, H.A., Khan, A.R., Naqvi, R.R., Malik, A., Shah, S.A., Khan, K., Hussain, G., 2001. Ambient air quality of two metropolitan cities of Pakistan and its health implications. Atmospheric Environment 35, 5971-5978.

Piñero García, F., Ferro García, M.A., Azahra, M., 2012. ^{7}Be behaviour in the atmosphere of the city of Granada January 2005 to December 2009. Atmospheric Environment 47, 84-91.

Piskunov, V.N., Golubev, A.V., Balashov, Y.S., Mavrin, S.V., Golubeva, V.N., Aleinikov, A.Y., Kovalenko, V.P., Solomatin, I.I., 2012. The effect of rain characteristics on scavenging rate of tritium-oxide from the atmosphere. Atmospheric Environment 62, 573-583.

Pszenny, A., Fischer, C., Mendez, A., Zetwo, M., 1993. Direct comparison of cellulose and quartz fiber filters for sampling submicrometer aerosols in the marine boundary layer. Atmospheric Environment. Part A. General Topics 27, 281-284.

Rahn, K.A., 1981. Relative importances of North America and Eurasia as sources of arctic aerosol. Atmospheric Environment (1967) 15, 1447-1455.

Ramanathan, V., Feng, Y., 2009. Air pollution, greenhouse gases and climate change:

Global and regional perspectives. Atmospheric Environment 43, 37-50.

Rindi, A., Charalambus, S., 1967. Airborne radioactivity produced at high-energy accelerators. Nuclear Instruments and Methods 47, 227-232.

Rozanski, K., Gonfiantini, R., Araguas-Araguas, L., 1991. Tritium in the global atmosphere: distribution patterns and recent trends. Journal of Physics G: Nuclear and Particle Physics 17, S523.

Samoli, E., Stafoggia, M., Rodopoulou, S., Ostro, B., Declercq, C., Alessandrini, E., Díaz, J., Karanasiou, A., Kelessis, A.G., Le Tertre, A., Pandolfi, P., Randi, G., Scarinzi, C., Zauli-Sajani, S., Katsouyanni, K., Forastiere, F., Group, M.P.S., 2013. Associations between fine and coarse particles and mortality in Mediterranean cities: results from the MED-PARTICLES project. Environmental health perspectives 121, 932-938.

Santschi, P.H., Hoehn, E., Lueck, A., Farrenkothen, K., 1987. Tritium as a tracer for the movement of surface water and groundwater in the Glatt Valley, Switzerland. Environmental Science & Technology 21, 909-916.

Sarmiento, J.L., 1983. A Simulation of Bomb Tritium Entry into the Atlantic Ocean. Journal of Physical Oceanography 13, 1924-1939.

Shimadera, H., Kondo, A., Kaga, A., Shrestha, K.L., Inoue, Y., 2009. Contribution of transboundary air pollution to ionic concentrations in fog in the Kinki Region of Japan. Atmospheric Environment 43, 5894-5907.

Solomon, D.K., Poreda, R.J., Schiff, S.L., Cherry, J.A., 1992. Tritium and helium: 3 as groundwater age tracers in the Borden Aquifer. Water Resources Research 28, 741-755.

Tadros, C.V., Hughes, C.E., Crawford, J., Hollins, S.E., Chisari, R., 2014. Tritium in Australian precipitation: A 50 year record. Journal of Hydrology 513, 262-

273.

Todd, J.F., Wong, G.T.F., Olsen, C.R., Larsen, I.L., 1989. Atmospheric depositional characteristics of beryllium 7 and lead 210 along the southeastern Virginia coast. Journal of Geophysical Research: Atmospheres 94, 11106-11116.

Tokuyama, H., Oonishi, M., 1997. Precipitation washout of tritiated water vapor from a nuclear reactor. Journal of Environmental Radioactivity 34, 59-68.

Turekian, K.K., Benninger, L.K., Dion, E.P., 1983. ^{7}Be and ^{210}Pb total deposition fluxes at New Haven, Connecticut and at Bermuda. Journal of Geophysical Research: Oceans 88, 5411-5415.

UNSCEAR, 1988. Sources, Effects and Risks of Ionizing Radiation. United Nation Scientific Committee on the Effects of Atomic Radiation, United Nations, New York.

UNSCEAR, 2000. Sources and Effects of Ionizing Radiation. United Nation Scientific Committee on the Effects of Atomic Radiation, United Nations, New York.

UNSCEAR, 2016. Biological Effects of Selected Internal Emitters—Tritium, in: Sources, Effects and Risks of Ionizing Radiation. United Nations Scientific Committee on the Effects of Atomic Radiation, United Nations, New York.

Vichot, L., Boyer, C., Boissieux, T., Losset, Y., Pierrat, D., 2008. Organically bound tritium (OBT) for various plants in the vicinity of a continuous atmospheric tritium release. Journal of Environmental Radioactivity 99, 1636-1643.

Von Buttlar, H., Wendt, I., 1958. Ground-water studies in New Mexico using tritium as a tracer. Eos, Transactions American Geophysical Union 39, 660-668.

Wallbrink, P.J., Murray, A.S., 1994. Fallout of ^{7}Be in South Eastern Australia. Journal of Environmental Radioactivity 25, 213-228.

Wang, J., Hu, Z., Chen, Y., Chen, Z., Xu, S., 2013. Contamination characteristics and possible sources of PM10 and PM2.5 in different functional areas of Shanghai, China. Atmospheric Environment 68, 221-229.

Wang, L., Jang, C., Zhang, Y., Wang, K., Zhang, Q., Streets, D., Fu, J., Lei, Y., Schreifels, J., He, K., Hao, J., Lam, Y.-F., Lin, J., Meskhidze, N., Voorhees, S., Evarts, D., Phillips, S., 2010. Assessment of air quality benefits from national air pollution control policies in China. Part II: Evaluation of air quality predictions and air quality benefits assessment. Atmospheric Environment 44, 3449-3457.

Yang, K.-L., 2002. Spatial and seasonal variation of PM10 mass concentrations in Taiwan. Atmospheric Environment 36, 3403-3411.

Yasunari, T.J., Yamazaki, K., 2009. Impacts of Asian dust storm associated with the stratosphere-to-troposphere transport in the spring of 2001 and 2002 on dust and tritium variations in Mount Wrangell ice core, Alaska. Atmospheric Environment 43, 2582-2590.

Yoo, J.-M., Lee, Y.-R., Kim, D., Jeong, M.-J., Stockwell, W.R., Kundu, P.K., Oh, S.-M., Shin, D.-B., Lee, S.-J., 2014. New indices for wet scavenging of air pollutants (O_3, CO, NO_2, SO_2, and PM10) by summertime rain. Atmospheric Environment 82, 226-237.

Yoshimori, M., 2005. Beryllium 7 radionucleide as a tracer of vertical air mass transport in the troposphere. Advances in Space Research 36, 828-832.

Zhang, X.Y., Gong, S.L., Shen, Z.X., Mei, F.M., Xi, X.X., Liu, L.C., Zhou, Z.J., Wang, D., Wang, Y.Q., Cheng, Y., 2003. Characterization of soil dust aerosol in China and its transport and distribution during 2001 ACE-Asia: 1. Network observations. Journal of Geophysical Research: Atmospheres 108.

Abstract (in Korean)

자연기원 또는 인간기원 방사성 핵종인, 삼중수소는 물을 구성하는 수소와 유사한 거동, 물리화학적 특성이 있고, ^{7}Be은 입차 친화적 특성을 보이기 때문에 대기권, 수권의 다양한 환경 프로세스 연구에 추적자로 널리 이용된다. 이 연구의 주요 목적은 다양한 대기환경 시료 중 삼중수소와 ^{7}Be의 조사를 통해, 1)지하수 연대측정에 중요하게 사용되는 빗물 중 삼중수소의 배경자료를 구축, 2)동북아시아 지역에서 미세입자 제거효율의 계절변동을 평가, 그리고 3)원자력발전소로부터 방출된 삼중수소의 확산 및 제거특성을 평가하는 것이다.

북미, 호주, 유럽, 남아시아를 포함한 다양한 지역에서 삼중수소의 시·공간적 분포특성에 대한 연구가 수행되었다. 그러나, 동북아시아 지역에서는 이러한 연구가 이루어 지지 않아 삼중수소의 분포에 대한 기본적인 정보가 구축되지 않았다. 이 연구에서는 1961년부터 한국의 16개 지점에서 측정된 빗물 중 삼중수소의 조사결과를 이용하여 시·공간적 분포특성 평가하였다. 한국에서 조사된 빗물 중 삼중수소의 농도는 1963년에 활발한 대기핵실험에 의해 최대값을 보였고, 점차 감소하여 2003년 이후에는 핵실험 이전 수준의 농도를 유지하고 있었다. 이 결과는 전세계에서 조사된 농도 변화 추세와 일치하였다. 1998년부터 2017년 까지 조사된 빗물 중 삼중수소는 봄에 성층권과 대류권의 활발한 기체교환에 의해 높은 농도를 보였고, 여름철 해양 대기의 유입에 의해 농도가 낮아지는 경향을 나타냈다. 빗물 중

삼중수소의 농도는 해수기원 수증기의 영향으로 연안에 가까워질수록 농도가 낮아졌다. 이 연구의 결과들은 동북아시아 지역을 대상으로 하는 지하수 연대 측정과 같은 수문학 연구의 중요한 배경자료로 사용될 수 있을 것으로 판단된다.

대기 미세입자의 계절변동 및 빗물에 의한 제거효율을 평가하기 위해 20년간 조사된 표층대기 입자와 강수 시료 중 ^{7}Be의 방사능 농도 분포를 분석하였다. 표층대기시료의 ^{7}Be 농도는 성층권과 대류권의 활발한 기체교환에 의해 봄에 높고, 강수에 의한 제거효과로 인해 여름에 낮은 경향을 보였다. 대기시료의 ^{7}Be의 농도는 강수량이 증가할수록 감소하여, 강수시료의 ^{7}Be의 농도는 강수량과 음의 상관관계를 보였다 (r^2=0.34). 대기시료 중 ^{7}Be의 농도는 PM10농도와 양의 상관관계를 나타냈다 (r^2=0.32). 이 결과는 ^{7}Be과 PM10의 농도는 강수에 의한 제거 효과에 큰 영향을 받는 다는 것을 나타낸다. 대기 및 강수시료 중 ^{7}Be의 분석결과를 바탕으로 계산된 대기 미세입자의 퇴적속도는 7월에 최대값 (1.9 cm s^{-1}) 을 보였고 3월에 최소값 (0.22 cm s^{-1}) 을 나타냈다. 이 결과는 만약 미세입자의 공급이 일정하다고 가정하면 겨울철 농도는 여름철보다 6배 높은 농도를 보일 수 있다는 것을 의미한다. 결론적으로 이 연구 결과들은 대기의 미세입자의 농도 변화는 강수에 의한 제거에 큰 영향을 받는다는 것을 나타낸다.

1998년부터 2015년 까지 월성원자력발전소 주변에서 수증기 및 강수 중 삼중수소 농도를 조사하였다. 수증기중 삼중수소의 농도는

2.2−2200 Bq/L, 강수중 삼중수소의 농도는 0.3−1090 Bq/L의 범위를 나타냈다. 여름철 수증기의 삼중수소 농도는 이 지역의 풍향 특성에 영향을 받아 봄에 가을과 겨울에 비해 7배 높은 값을 보였다. 수증기와 강수시료 중 삼중수소의 연평균 농도는 연간 원자력발전소에서 방출하는 삼중수소의 양에 따라 각각 56%와 83% 수준 내에서 변동했다. 수증기와 강수 중 삼중수소의 농도는 원자력발전소로부터 멀어질수록 급격하게 감소하는 경향을 보였다. 원자력발전소에서 방출되는 삼중수소의 약 0.5−30%가 발전소 주변 30 km반경 내에서 강수에 의해 지표면으로 제거되었고, 제거되는 양은 강수량에 비례하였다. 결론적으로 원자력발전소 주변 삼중수소의 농도분포는 풍향, 강수량 그리고 원자력발전소의 삼중수소 방출량에 영향을 받는 것으로 나타났다.